DOI: 10.1002/chem.200601136

Latrunculin Analogues with Improved Biological Profiles by "Diverted Total Synthesis": Preparation, Evaluation, and Computational Analysis

Alois Fürstner,*[a] Douglas Kirk,[a] Michaël D. B. Fenster,[a] Christophe Aïssa,[a] Dominic De Souza,[a] Cristina Nevado,[a] Tell Tuttle,[a] Walter Thiel,[a] and Oliver Müller[b]

Abstract: Deliberate digression from the blueprint of the total syntheses of latrunculin A (**1**) and latrunculin B (**2**) reported in the accompanying paper allowed for the preparation of a focused library of "latrunculin-like" compounds, in which all characteristic structural elements of these macrolides were subject to pertinent molecular editing. Although all previously reported derivatives of **1** and **2** were essentially devoid of any actin-binding capacity, the synthetic compounds presented herein remain fully functional. One of the designer molecules with a relaxed macrocyclic backbone, that is compound **44**, even surpasses latrunculin B in its effect on actin while being much easier to prepare. This favorable result highlights the power of "diverted total synthesis" as compared to the much more widely practiced chemical modification of a given lead compound by conventional functional group interconversion. A computational study was carried out to rationalize the observed effects. The analysis of the structure of the binding site occupied by the individual ligands on the G-actin host shows that latrunculin A and **44** both have similar hydrogen-bond network strengths and present similar ligand distortion. In contrast, the H-bond network is weaker for latrunculin B and the distortion of the ligand from its optimum geometry is larger. From this, one may expect that the binding ability follows the order **1** $\geq$ **44** $>$ **2**, which is in accord with the experimental data. Furthermore, the biological results provide detailed insights into structure/activity relationships characteristic for the latrunculin family. Thus, it is demonstrated that the highly conserved thiazolidinone ring of the natural products can be replaced by an oxazolidinone moiety, and that inversion of the configuration at C16 (latrunculin B numbering) is also well accommodated. From a purely chemical perspective, this study attests to the maturity of ring-closing alkyne metathesis (RCAM) catalyzed by a molybdenum alkylidyne complex generated in situ, which constitutes a valuable tool for advanced organic synthesis and natural product chemistry.

Keywords: actin · chemical biology · computational chemistry · macrolides · metathesis · total synthesis

Introduction

Incubation of eukaryotic cells with low micromolar concentrations of the marine natural product latrunculin A (**1**) or its ring-contracted congener latrunculin B (**2**) results in the rapid disassembly of the actin cytoskeleton.[1,2] In terms of specificity and efficacy, this effect is reminiscent of genetic knockout experiments that inactivate a single cellular constituent. As a result, the latrunculins enjoy widespread use as probe molecules in chemical biology;[3] however, their mode of action is by no means fully understood, not least because insights into structure/activity relationships (SAR) are missing. This lack of information is due, in part, to the fact that essentially all post facto chemical modifications of **1** and **2** engendered a complete loss of their physiological activity.[4]

Actin, as the most abundant protein, determines the shape and mechanical properties of eukaryotic cells, effects cell locomotion and strength development in muscles, and is involved in motility processes as fundamental as cytokinesis, exocytosis and endocytosis.[5] The latrunculins are known to

[a] Prof. A. Fürstner, Dr. D. Kirk, Dr. M. D. B. Fenster, Dr. C. Aïssa, Dr. D. De Souza, Dr. C. Nevado, Dr. T. Tuttle, Prof. W. Thiel
Max-Planck-Institut für Kohlenforschung
45470 Mülheim/Ruhr (Germany)
Fax: (+49) 208-306-2994
E-mail: fuerstner@mpi-muelheim.mpg.de

[b] Univ.-Doz. O. Müller
Max-Planck-Institut für Molekulare Physiologie
44227 Dortmund (Germany)

Supporting information for this article is available on the WWW under http://www.chemeurj.org/ or from the author.

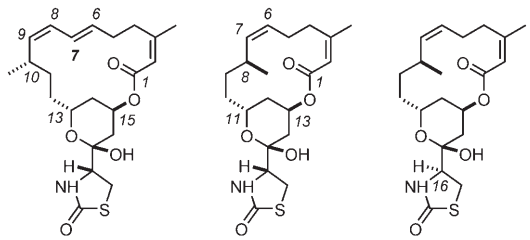

form 1:1 complexes with the actin monomers (globular actin, G-actin) that are incapable of polymerizing to the intact protein filament network (fibrous actin, F-actin). Their binding site is located near the nucleotide binding cleft between the four subdomains of the protein and was structurally characterized at 2 Å resolution by crystal structure analysis of latrunculin A (**1**) bound to its protein host (Figure 1).[6,7] This investigation indicates that binding of **1** exploits the very mobility of the protein loops of G-actin, thereby influencing critical subdomain contacts at a minimal penalty to its own ligation near the better ordered base of the cleft.

A more detailed analysis of the interactions between **1** and G-actin reveals several noteworthy features: While the 2-thiazolidinone group fits neatly into the binding pocket, it does *not* seem to engage its conspicuous sulfur atom in the hydrogen bond network formed by the other heteroelements.[8] Specifically, the S atom does not entertain any immediate interactions below 4 Å except for an intramolecular bond to the C17 hydroxy group (3.478 Å) of its own backbone. The two other closest residues are a water molecule (4.084 Å) and R206 of the protein (4.054 Å). This abstinence of the sulfur atom is highly surprising if one considers that the 2-thiazolidinone ring constitutes an otherwise unknown structural motif in nature but is so prominently featured throughout the entire latrunculin family.[2]

Furthermore, the crystal structure shows the fit between the macrocyclic loop of **1** and the hydrophobic region of the binding site, even though the hydrocarbon chain from C5 to C7 forms only few contacts and is partly exposed to solvent.[6] This may explain why nature has evolved the ring contracted congener latrunculin B (**2**) missing one of the double bonds alongside with latrunculin A (**1**) as a similarly potent actin binder.

The published crystal structure[6] can also be interrogated in stereochemical terms. Thus, the configuration of C16 determines the orientation of the thiazolidinone ring relative to its hydrogen bonding partners and may hence affect the binding constant. Under this premise it is surprising that a recent collection of the producing sponge *Negombata magnifica* has led to the isolation of small amounts of 16-*epi*-latrunculin B (**3**), which differs from all other members of this family in the absolute stereochemistry at this particular site.[9] Unfortunately, however, the actin-binding capacity of **3** was not reported, even though it is known that this compound retains significant cytotoxicity and exhibits antiviral properties as well.

The information gathered from the crystal structure analysis of **1** bound to G-actin is graphically summarized in Figure 2. From this, it seems highly likely that modifications of the chemically accessible heteroelements will disrupt the tight hydrogen bonding pattern, which may explain why previous attempts to improve actin binding by derivatization of **1** or **2** essentially met with failure.[4a] Rather, we presumed that meaningful SAR-studies should focus on the elucidation of the role of the sulfur atom, the macrocyclic frame, and the chiral center C16. Any such structural editing, however, is difficult to achieve if one starts from the natural products themselves; de novo synthesis seems to be much more appropriate to garner relevant insights. Because our total syntheses of **1**–**3** reported in the accompanying paper are flexible by design,[11] we felt in a strong position to venture into such an endeavor at the chemistry/biology interface. The results of our "diverted total synthesis"[12] campaign are summarized below.[13]

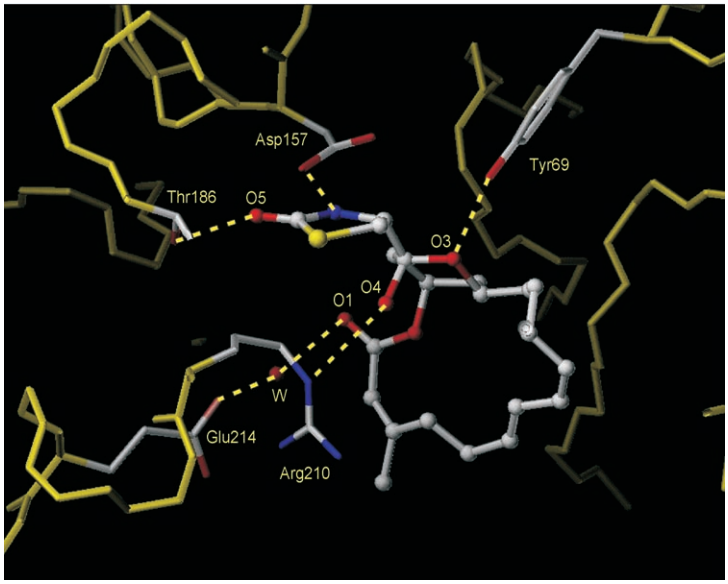

Figure 1. Pertinent part of the crystal structure of the G-actin/latrunculin A (**1**) complex, together with the putative hydrogen-bonding network responsible for ligand binding according to ref. [6].

Results and Discussion

Preparation of a focussed library: Our total syntheses of latrunculin A (**1**), its ring contracted congener latrunculin B (**2**) and the recently discovered 16-*epi*-analogue **3** hinge upon

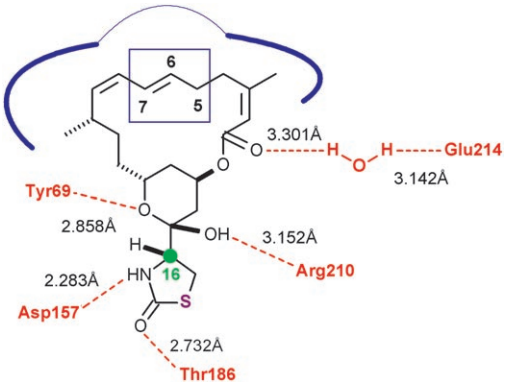

Figure 2. Graphical summary of the putative bonding situation between latrunculin A (**1**) and G-actin as evident from the crystal structure analysis reported in ref. [6], together with the published hydrogen bond lengths.[10]

the convergent assembly of these targets from three building blocks and are therefore inherently modular.[11–14] Since the individual components are readily amenable to structural modification, the underlying synthesis blueprint might allow for the preparation of a focused library of analogues adequate for investigations of the structural requirements for actin binding.

To this end, a matrix of four heterocyclic building blocks **4**–**7**, five acid segments **8**–**12**, and two different aldehyde components **13** and **14** was prepared that allow for the assembly of a sizeable number of "latrunculin-like" macrolides via the established routes (Figure 3).[13,14] The heterocyclic ketones were chosen to address the specific role, if any, of the sulfur atom and should also reveal whether the configuration of C16 correlates with biological activity. The different acid parts allow one to fine-tune the lipophilicity of the compounds and to modulate the rigidity of the macrocyclic perimeters. Their syntheses (Schemes 1 and 2) followed

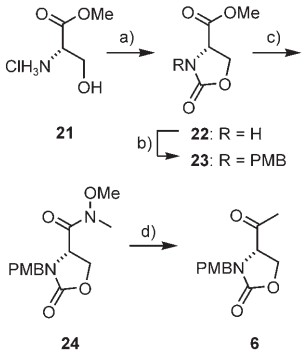

Scheme 1. a) Triphosgene, Et_3N, CH_2Cl_2, 0 °C, 99 %; b) PMBBr, NaH, THF, −15 °C, 56 %; c) i) KOH, 1,4-dioxane/H_2O, 97 %; ii) (MeO)-MeNH·HCl, (benzotriazol-1-yloxy)tris-(dimethylamino)phosphonium hexafluorophosphate (BOP), Et_3N, CH_2Cl_2, 99 %; d) MeMgBr, THF, −40 °C, 96 % (*ee* 77 %, crude), then recrystallization form *tert*-butyl methyl ether, *ee* ≥ 97 %.

established routes, with the use of cheap, non-toxic and benign [Fe(acac)$_3$] as catalyst in the cross coupling step leading to **9** being particularly noteworthy.[15]

With regard to the aldehyde segment, the methyl branch at C8 (Lat-B numbering) was removed in synthon **14** relative to the parent compound **13**. This seemingly minor modification pays off in preparative terms since access to **14** required only three high yielding steps starting from 5-heptynal **29** and is easily scaleable (Scheme 3).

The assembly process followed the protocols developed in the total synthesis of **1**–**3** as described in detail in the accompanying paper,[11] although not all steps were fully optimized for each individual analogue prepared during this campaign. A representative case is outlined in Scheme 4. Thus, the titanium aldol reaction[16] of the serine derived ketone **7** with the "nor-methyl" aldehyde **14** gave alcohols **32** and **33** in a 1.1:1 ratio which were separable by flash chromatography. The stereochemi-

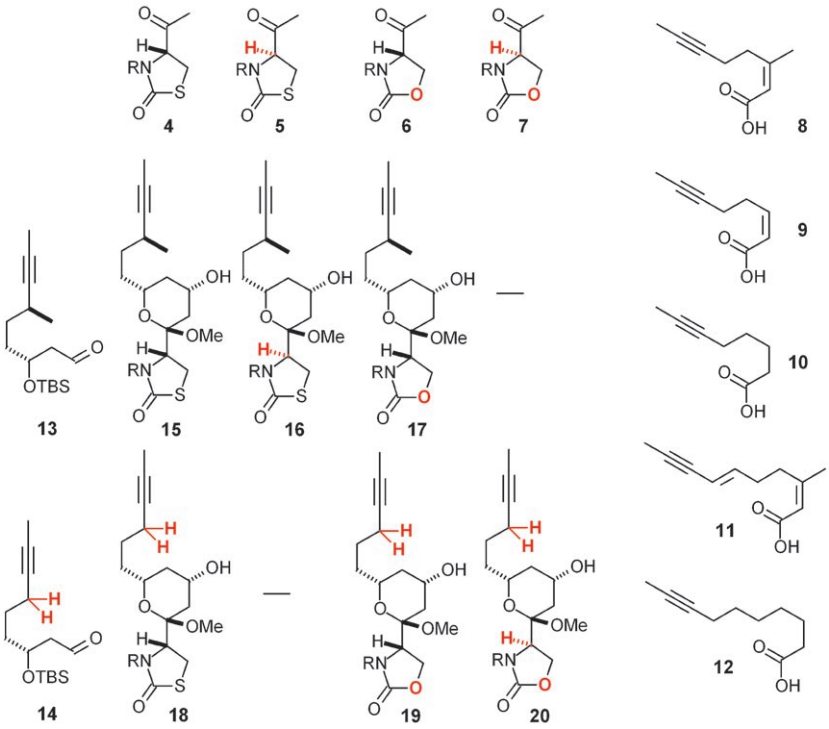

Figure 3. Matrix of building blocks used for the preparation of the latrunculins and analogues. Structural modifications relative to the parent natural products are color-coded in red.

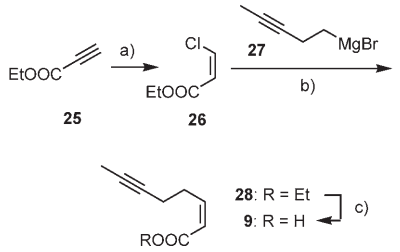

Scheme 2. a) LiCl, HOAc, MeCN, reflux, 60%; b) [Fe(acac)$_3$] (10 mol%), THF, −30°C, 78%; c) NaOH, MeOH, 74%.

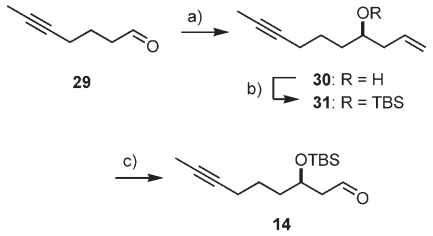

Scheme 3. a) (−)-Ipc$_2$B(allyl), Et$_2$O, −100°C; b) TBSCl, imidazole, DMF, 68% (over both steps); c) O$_3$, MeOH, then PPh$_3$, 67%.

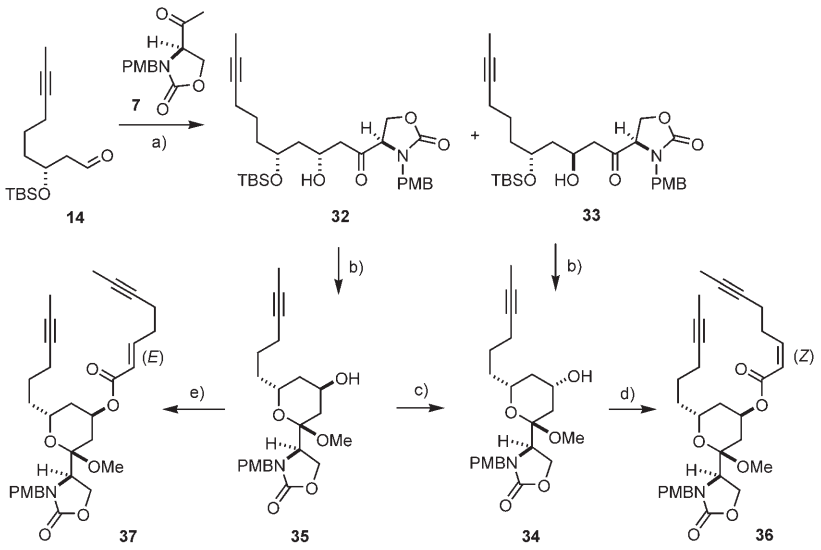

Scheme 4. a) TiCl$_4$, (*i*Pr)$_2$NEt, CH$_2$Cl$_2$, −78°C, 58% (d.r. 1.1:1); b) i) aq. HCl (1 M), THF; ii) MeOH, CSA cat., **34** (92%), **35** (88%); c) i) diisopropyl azodicarboxylate (DIAD), *p*-nitrobenzoic acid, THF; ii) K$_2$CO$_3$, MeOH/H$_2$O, 49% (over both steps); d) i) Tf$_2$O, pyridine, CH$_2$Cl$_2$, −78 → −45°C; ii) sodium salt of acid **9**, [15]crown-5, THF, 0°C → RT, 70%; e) 2,4,6-trichlorobenzoic acid chloride, Et$_3$N, acid **9**, DMAP cat., toluene, 71%.

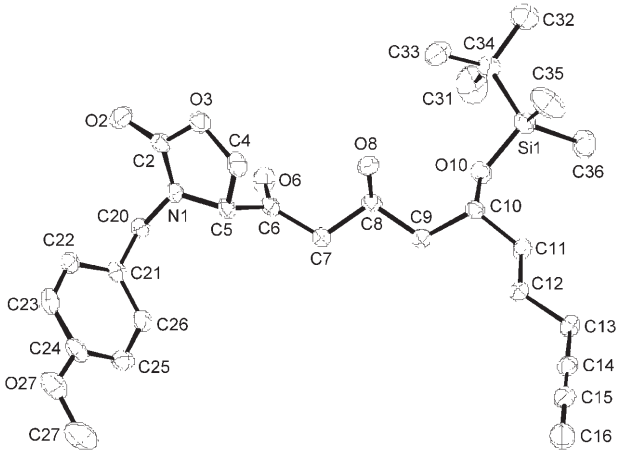

Figure 4. Molecular crystal structure of compound **33** in the solid state. Anisotropic displacement parameters are drawn at the 50% probability level.

cal assignment was unambiguous on the basis of a crystal structure analysis of the minor product (Figure 4).

The two stereomers were processed separately by acid catalyzed cleavage of the TBS groups, leading to the spontaneous cyclization of the corresponding tetrahydropyran rings which were locked as methyl glycosides. Compound **34** was then converted into diyne **36** as the substrate for the envisaged ring-closing alkyne metathesis (RCAM) via the corresponding triflate.[11,14] Since attempted conversion of the diastereomeric alcohol **35** into diyne **36** under Yamaguchi conditions[17] led to the concomitant isomerization of the (*Z*)-configured α,β-unsaturated carboxylic acid **9** with formation of the thermodynamically more stable (*E*)-configured ester **37**,[18] the secondary hydroxy group of **35** was inverted by means of a Mitsunobu reaction/saponification sequence,[19] thereby ensuring convergence of the assembly line.

Cyclization of **36** by ring-closing alkyne metathesis (RCAM)[20,21] proceeded smoothly, affording cycloalkyne **38** in 71% yield, provided that the molybdenum complex [Mo{N(*t*Bu)(Ar)}$_3$] (**40**, Ar = 3,5-dimethylphenyl) activated in situ with CH$_2$Cl$_2$, as previously described by our group,[22] was used as the catalyst (Scheme 5); in striking contrast, attempted cyclization with the aid of the Schrock alkylidyne [(*t*BuO)$_3$W≡CCMe$_3$] (**41**)[23] met with failure, thus attesting to the superior functional group compatibility of the molybdenum-based system. Final Lindlar hydrogenation of cycloalkyne **38** followed by global deprotection of the resulting alkene with cerium ammonium nitrate (CAN) furnished product **39** in good overall yield. This particular compound differs from latrunculin B (**2**) in three structural aspects: it contains a peripheral oxazolidin-2-one rather than a thiazolidin-2-one ring, shows the opposite configuration at the attachment point C16, and lacks the two methyl branches on the macrocyclic loop. A number of related, fully synthetic "latrunculin-like" products were prepared analogously (Figure 5) with

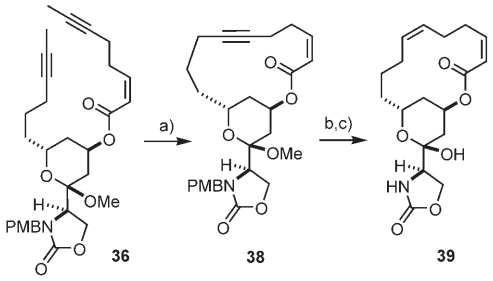

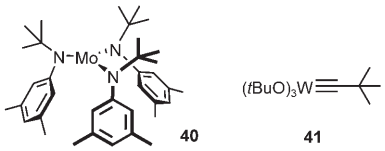

Scheme 5. a) Complex **40** (25 mol%), toluene/CH_2Cl_2, 80°C, 71%; b) H_2 (1 atm), Lindlar catalyst, CH_2Cl_2, quant.; c) CAN, MeCN/H_2O, 93%.

the structural changes relative to the parent latrunculins being highlighted in red for easier survey.

Additional compounds for testing were obtained by "premature escape" from the assembly line. Specifically, derivative **48** representing the "alkynylogous" congener of latrunculin B (**2**) was accessible by deprotection of cycloalkyne **53** as the key intermediate of our total synthesis of **2** (Scheme 6).[11,14] Due to its very strained bicyclic edifice, however, this compound had only a limited lifetime. To address the question whether a macrocyclic backbone is necessary at all for actin binding, analogues **50** and **51** were prepared from building blocks **18** and **17**,[13] respectively, by the standard esterification/deprotection manifold (Scheme 7). Finally, the bare macrocycle **52** devoid of the entire heterocyclic domain present in latrunculin B was prepared as a "negative control" for the bioassay on treatment of diyne **56** with the molybdenum catalyst **40** in toluene/CH_2Cl_2 under

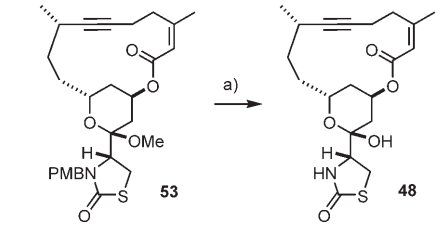

Scheme 6. a) CAN, MeCN/H_2O, 80%.

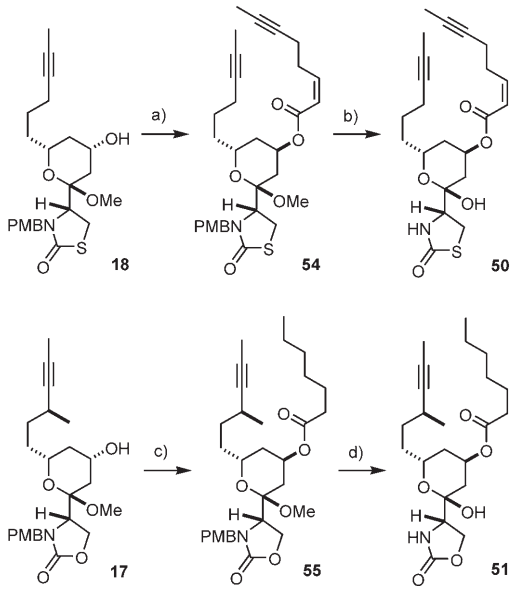

Scheme 7. a) Acid **9**, diethyl azodicarboxylate (DEAD), PPh_3, benzene, 61%; b) CAN, MeCN/H_2O 2:1, 49%; c) heptanoic acid, DEAD, PPh_3, benzene; d) CAN, MeCN/H_2O 2:1.

the usual conditions, followed by Lindlar hydrogenation of the resulting cycloalkyne **57** (Scheme 8).

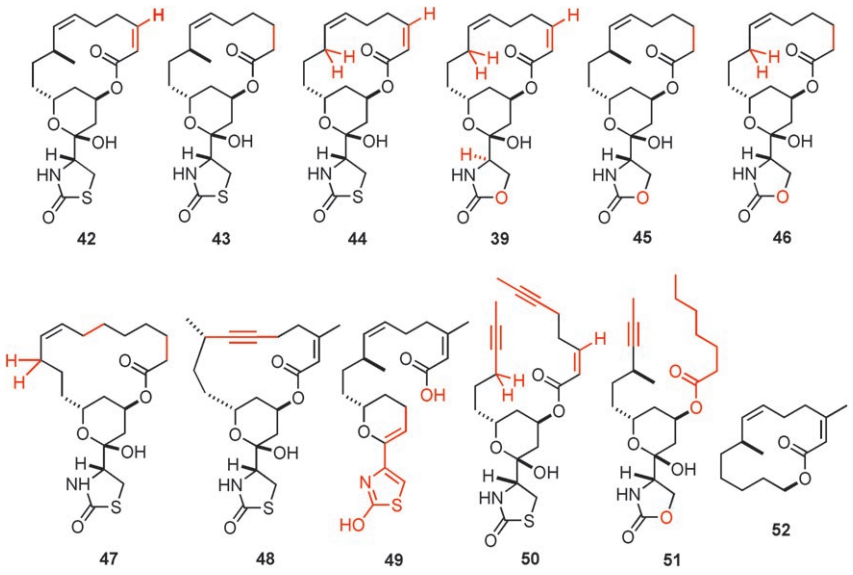

Figure 5. Collection of fully synthetic latrunculin analogues used for the actin-binding assays.

Evaluation of the actin-binding properties: It is well established in the literature that incubation of non-muscular cells with **1** or **2** leads to almost instantaneous morphological changes and shape malformations, which constitute a convenient phenomenological read-out for actin binding.[1,3] This type of assay was used for the evaluation of the compounds prepared above using the NIH3T3 fibroblast cell-line. The actin cytoskeleton of these cells was visualized by staining with fluorescence-marked phalloidin, whereas their nuclei were stained in blue with 2-(4-amidinophenyl)-

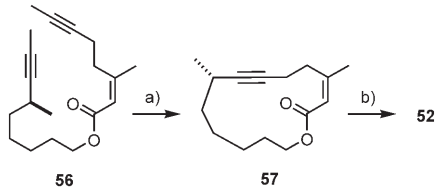

Scheme 8. a) Complex **40** (10 mol %), toluene/CH_2Cl_2, 80 °C, 70 %; b) H_2 (1 atm), Lindlar catalyst, CH_2Cl_2, 70 %.

6-indolecarbamidine hydrochloride (DAPI) (Figure 6, micrograph I).

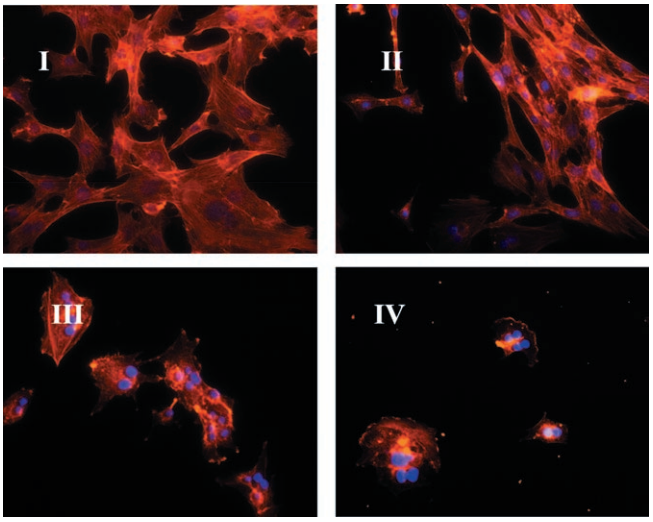

Figure 6. Fluorescence micrographs (250×) of NIH3T3 fibroblast cells show that compound **44** exerts a stronger effect than the natural product Lat-B (**2**). The actin filament is stained with fluorescence-marked phalloidin, the nuclei with DAPI. **I**: untreated; **II**: after incubation with **2** (5 μM); **III**: after incubation with **44** (5 μM); **IV**: after incubation with **44** (10 μM).

In accordance with literature data,[1,3] latrunculin A (**1**) turned out to be more effective than its ring contracted congener latrunculin B (**2**). After this calibration of the assay, all novel analogues were screened at different concentrations. Representative micrographs are depicted in Figures 6 and 7, and the resulting semi-quantitative data are summarized in Table 1.

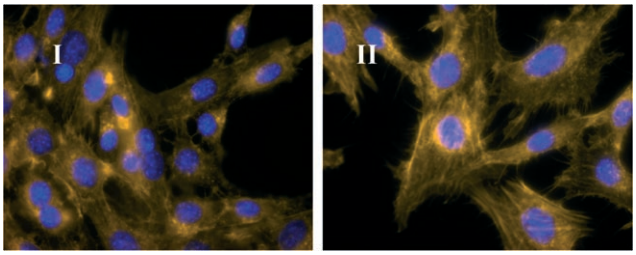

Figure 7. Fluorescence micrographs (250×) showing the effect of synthetic latrunculin derivatives on NIH3T3 fibroblasts: **I**: after incubation with 16-*epi*-LAT B (**3**) (5 μM); **II**: after incubation with **39** (5 μM).

Table 1. Microfilament disrupting activity of Lat-A (**1**), Lat-B (**2**), 16-*epi*-Lat-B (**3**), and their fully synthetic analogues.[a]

Compound	Effective concentration		
	1 μM	5 μM	10 μM
1	+	++	+++
44	+	±+	±++
42	±	+	++
2	–	+	++
39	–	+	±+
3	–	±	+
43	–	±	+
45	–	±	+
46	–	±	+
47	–	±	+
48	–	–	+
50	–	–	±
51	–	–	±
49	–	–	–
52	–	–	–

[a] Abbreviations: –, no effect; ±, weak effect: unaltered cell number, intact cell morphology, filamentous and slightly disrupted actin; +, significant effect: less than 80 % viable cells, spindle-shaped cell morphology, filamentous and disrupted actin ; ++, strong effect: less than 50 % viable cells, poly-nuclear cells, more disrupted than filamentous actin; +++, very strong effect: less than 20 % viable cells, poly-nuclear, rounding and isolated cells, disrupted actin (compare representative micrographs in Figure 6).

As can be seen from this compilation, all macrocyclic compounds, except the bare lactone **52** devoid of the heterocyclic domain, were found to induce depolymerization of F-actin at 10 μM concentration. Thus, the implemented structural modifications are well accommodated and the non-natural analogues remain functional. This result is highly significant if one recalls that virtually all post-facto chemical modifications of the latrunculins previously reported in the literature resulted in a complete loss of actin depolymerization capacity.[4]

A closer look at the data set reveals further salient features. Most strikingly, removal of the seemingly unfunctional methyl branches at C3 and/or C8 of the macrocyclic ring of **2** leads to a significant increase in potency. As evident from the micrographs shown in Figure 6, the bis-*nor*-Lat-B derivative **44** clearly surpasses the parent compound latrunculin B (**2**) in its effect on actin, reaching a potency previously known only for latrunculin A as the most active natural product of this series (cf. Table 1). This noteworthy result has important implications: Since **44** is much easier to prepare than both **1** and **2** by a route that has only 11 steps in the longest linear sequence,[13] this particular analogue may become available through total synthesis in sufficient quantity at a competitive price and might therefore help to ensure a constant supply of a fully functional and highly potent actin-binding probe molecule. Access to the natural latrunculins by harvesting and extracting the producing sponge is limited and gets increasingly difficult because *Negombata magnifica* populates the highly sensitive and protected ecosystem of the coral reefs of the Red Sea.[24]

The other structural modifications engender a slight decrease in activity. Specifically, all compounds belonging to

the 16-*epi*-series are somewhat less active than their parent analogues. This includes naturally occurring 16-*epi*-latrunculin B (**3**)[9] which is inferior to latrunculin B (**2**) (Figure 7) and significantly less effective than the best of our novel analogues. Overall, the following ranking was observed: Lat-A (**1**) $\geq$ **44** $>$ **42** $\geq$ Lat-B (**2**) $>$ 16-*epi*-Lat-B (**3**).

Comparison of the "latrunculins" bearing the natural 2-thiazolidinone ring with their respective 2-oxazolidinone analogues reveals yet another important aspect. Although somewhat less potent, all compounds of the latter series retain significant bioactivity. This result corroborates the notion that the presence of the sulfur atom is not essential for actin binding as we had anticipated from the analysis of the bonding situation observed in the **1**/G-actin co-crystals (see above). The best oxazolidinone-containing analogue **39** exhibits an activity that exceeds that of the natural product 16-*epi*-latrunculin B (**3**)[9] but is weaker than that of **1** or **2** (cf. Figure 7). Whether the slight decrease in potency in going form the S- to the O-series is due to the larger size and better polarizibility of the sulfur atom or to modulations of other physicochemical properties remains yet to be elucidated. What is even more remarkable, however, is the finding that all 2-oxazolinone containing derivatives investigated are markedly less cytotoxic than their relatives of the 2-thiazolidinone series. Specifically, 100% of the NIH3T3 fibroblasts were alive after 24 h of incubation with 10 μM solutions of either **39** or **45**, whereas even a concentration of 5 μM of **1** or **2** kills $>$ 50% of the cultured cells during the same time.

While the data outlined above indicate that the latrunculins can accommodate substantial structural editing without loss of their physiological properties and may even lead to improved biological profiles, opening of the macrocycle is largely detrimental. Thus, formal "cleavage" of the macrocylic edifice as realized in **50** and **51** leaves only weak actin-binding properties behind. Likewise, the previously unknown degradation product of latrunculin B, that is compound **49**,[11] did not induce any noticeable morphological changes in the fibroblast cell culture.

Computational study: The biological activities of the different analogues summarized above suggest a difference in their binding abilities to G-actin. Therefore a computational study was carried out to investigate the structure of the binding site with bound latrunculin A (**1**) and consider the changes that occur in the presence of the smaller homologue latrunculin B (**2**) and the most potent of the fully synthetic analogues, that is, compound **44**. These three ligands show various levels of activity (**1** $\geq$ **44** $>$ **2**) and the aim of this study was to rationalize this experimental ranking.

The structure of actin with bound **1**, available from the protein data bank (PDB ID: 1ESV),[6] was used as the starting point for the computational study. A conformational search was performed for **1** and two of its analogues, **2** and **44**, at the semi-empirical level of theory and the resulting structures were subsequently optimized at the DFT level. The conformers were then docked into the actin-binding site and the complex with the best binding energy from each docking simulation was pre-minimized in CHARMM.[25–27] The structures resulting from the force field minimization were optimized at the hybrid quantum mechanical/molecular mechanical (QM/MM) level of theory with the modular program package CHEMSHELL.[28,29] The QM energy and gradients were provided by MNDO99,[30] with MNDO/H[31,32] as the QM level of theory. CHEMSHELL's internal force field driver supplied the MM energy and gradients, using the CHARMM parameter and topology data.[33–35] No electrostatic cut-offs were employed in the QM/MM calculations. Electrostatic embedding[36] with the charge-shift scheme[29,37] was used to couple the QM and MM regions. Full details of the computational methodology employed in this study are available in the Supporting Information.

In the following discussion of the binding of **1** and its analogues to actin we focus only on the most stable orientation of the ligand in the binding site, that is, on the complex with the lowest QM/MM energy after optimization (see Supporting Information for details). The computed binding site of the **1**/G-actin complex has a H-bond network similar but not identical to that of the crystal structure (PDB ID: 1ESV).[6] The backbone RMSD of the two structures is 1.2 Å, with the main deviations occurring for surface residues. However, all tertiary structural features are maintained and the general overlap of the structures is good (Figure 8).

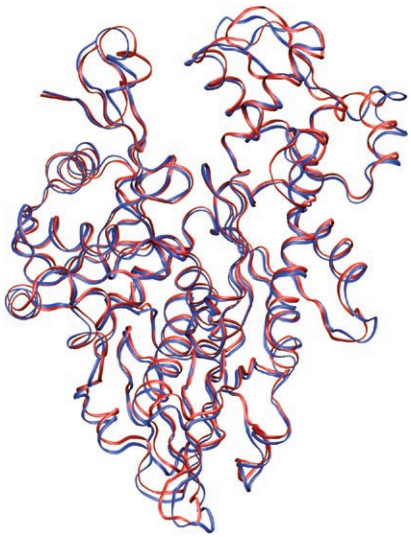

Figure 8. Overlap of the crystal structure backbone (blue) and the optimized **1**/G-actin complex backbone (red).

The latrunculin A ligands from the optimized complex and the crystal structure match well (Figure 9a). However, the optimization of the binding site results in some changes in the H-bond network relative to the crystal structure due to missing side-chains. In the original PDB structure the side-chain of Glu207 was not resolved, and thus an interaction between the OH group of **1** and the NH group of Arg210 was listed as a stabilizing interaction. In the opti-

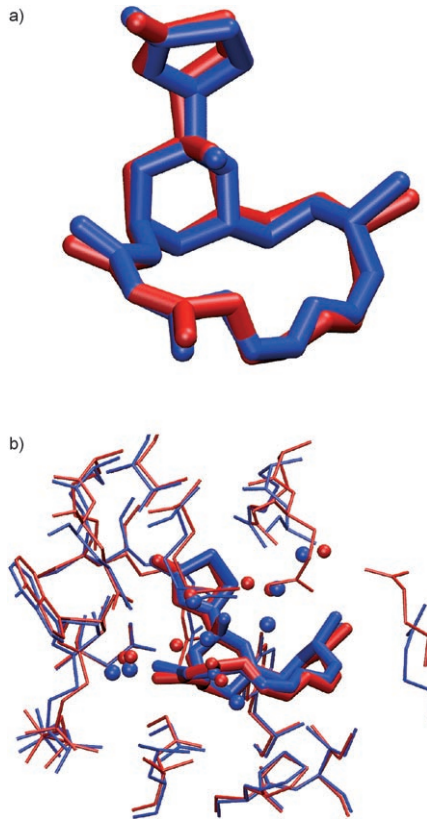

Figure 9. a) Overlap of the crystal (blue) and optimized (red) latrunculin A (**1**) residue in the binding site of G-actin; b) overlap of the residues forming the binding site for the crystal (blue) and optimized (red) complexes; the blue and red spheres represent oxygen atoms of water molecules.

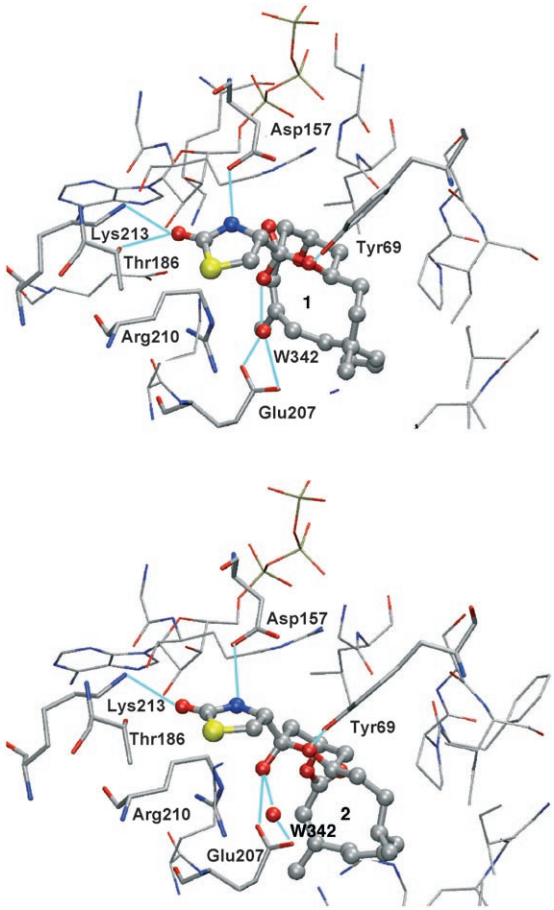

Figure 10. H-bond network of **1** (top) and **2** (bottom) in the actin-binding site after the QM/MM optimization.

mized structure, the side-chain of Glu207 is present and its carboxylate oxygen atom interacts strongly (r(H···O) = 1.77 Å) with the NH of Arg210. The OH group of **1** is able to form a strong hydrogen bond to one of the crystal waters, which in turn binds to the carboxylate O atoms of Glu207. There are also changes in the water positions around the binding site (spheres in Figure 9b). However, these have no effect on the H-bond network of the complex and are predominantly caused by a lack of strong H-bond partners (e.g., outside the binding site). Given the generally good overlap of the optimized and crystallographic binding site structures, and the problems with the unresolved side-chains in the latter, we consider the computed structure to be a reliable representation of the complex.

In the optimized binding site of the **1**/G-actin complex (Figure 10, top) there are strong H-bonds between the head-group of **1** and the surrounding residues (Table 2), while the macrocycle has no obvious H-bond pairing with the protein.[38] In the head-group, the NH and CO moieties form strong H-bonds to Asp157 and Thr186, respectively, while there exists only a weak interaction with Lys213. The O-atom of the tetrahydropyran ring forms a strong H-bond with Tyr69.

The binding site of the **2**/G-actin complex (Figure 10, bottom) has a similar, but weaker H-bond network compared with the complex formed by **1**. Considering the 2-thia-

Table 2. Hydrogen bonds between the ligands and the actin-binding site; $r = r_{\text{H-Xacc}}$ refers to the bond length [Å], $\alpha = \alpha_{\text{Y-H-Xacc}}$ to the bond angle [°].

Head-group	H-Bond[a]	**1**		**2**		**44**	
		r	α	r	α	r	α
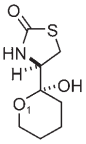	NH···Asp157	1.58	176	1.63	159	1.60	175
	CO···Thr186	1.73	167	–	–	–	–
	CO···Lys213[b]	–	–	–	–	1.73	157
	O1···Tyr69	1.94	163	2.00	156	1.98	154
	OH···Glu207	–	–	2.01	146	–	–

[a] Criterion adopted for a hydrogen bond: $r_{\text{H-Xacc}} \leq 2.5$ Å and $\alpha_{\text{Y-H-Xacc}} \geq 140°$. The putative hydrogen bonds forming the water bridge between the acyl group of latrunculin A and Glu214[10] are way beyond these thresholds and are therefore not considered further. Similarly weak interactions are present in the computed complexes **2**/G-actin and **44**/G-actin. [b] For **1** and **2** the interaction with Lys213 is present but weak ($r_{\text{H-Xacc}} \approx 2.6$ Å and $\alpha_{\text{Y-H-Xacc}} \approx 130°$).

zolidinone ring and the surrounding residues the strong NH group binding to Asp157 persists, but the strong H-bond between the CO group and Thr186 is lost, with only the weak interaction to Lys213 retained (Table 2). The H-bond between the oxygen atom of the tetrahydropyran ring and Tyr69 is slightly weaker compared to the analogous H-bond in the **1**/G-actin complex; however, an additional H-bond between the OH group and Glu207 exists in the **2**/G-actin complex, which will partially compensate for the other losses. Overall, the result is a weaker H-bond network with the two strong and one average H-bond in the **1**/G-actin complex being exchanged for one strong and two average H-bonds in the **2**/G-actin complex.

The H-bond network in the **44**/G-actin complex binding site (Figure 11) is different from the **1**/G-actin complex but is expected to be of a similar strength. The strong H-bond between the carbonyl and Thr186 (Table 2) is lost; however, this loss is offset by a strong ionic interaction with Lys213. The other dominant H-bonds in the **1**/G-actin complex (NH···Asp157 and O1···Tyr69) are essentially unchanged. Thus, although there is a shift in the binding pattern for the **44**/G-actin complex, the qualitative strength of the H-bonds (two strong and one average) remains similar to the parent complex.

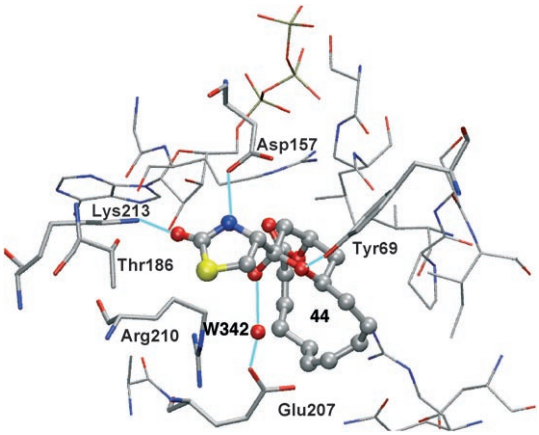

Figure 11. H-bond network of **44** in the actin-binding site after the QM/MM optimization.

The changes in the H-bond network hence offer a qualitative explanation for the observed differences in the biological activity of the three ligands. However, the contributions of the hydrophobic effect will also aid in stabilizing the ligands in the binding site. In accordance with the published crystal structure analysis,[6] the computational analysis shows that only a part of the macrocycle of latrunculin A (**1**) enjoys contacts to a hydrophobic environment, whereas the rest is solvent exposed or surrounded by polar substituents. Although the estimated hydrophobic contribution to the stability of the complex is higher for **1** than for its smaller congener **2** and the synthetic analogue **44**, no clear distinction between the three ligands is possible (for details, see Supporting Information).

The individual binding energy of the substrates can in principle be calculated directly. However, binding potential energies generally overestimate the binding free energy of a ligand to the receptor (which is measured experimentally) due to the neglect of the dynamic factors that influence the binding ability of ligands. Nonetheless, assuming that entropic and desolvation effects are approximately equivalent for the three ligands, the *relative* binding potential energies ($\Delta\Delta E_{bind}$) may be reasonable tools to compare binding abilities between the ligands.[39] In fact, they could be calculated as the difference between the relative stability of the ligand-enzyme complexes (ΔE_{isoR}) and of the free ligands in the gas phase (ΔE_{isoL}) (Scheme 9).

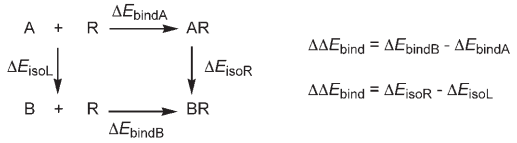

Scheme 9. Thermodynamic cycle for calculating relative binding energies.

$\Delta\Delta E_{bind}$ for the ligands can be determined from the homodesmotic reactions defined in Scheme 10. The **2**/G-actin complex is destabilized by 12.5 kcal mol^{-1} and the **44**/G-actin complex by 7.5 (= 12.5–5.0) kcal mol^{-1}, relative to the **1**/G-actin complex. Considering the isolated ligands, we find that **2** and **44** are destabilized by 2.3 and 1.2 kcal mol^{-1} rela-

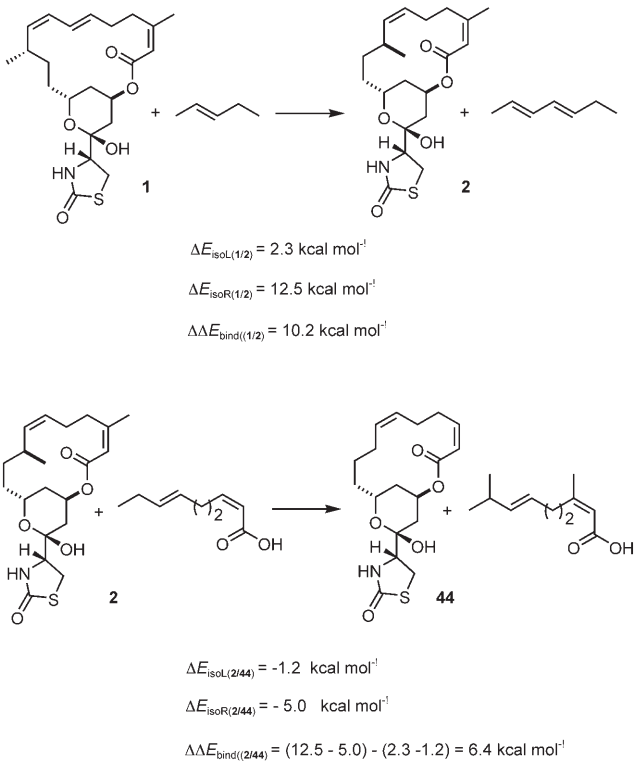

Scheme 10. Computed homodesmotic reactions for comparing the stability of **1** to **2**, and **2** to **44**. The partners in the isodesmic reactions (pent-2-ene, hept-2,4-diene, nona-2,6-dienoic acid, and 3,8-dimethyl-2,6-dienoic acid) were optimized in the gas phase (QM = MNDO/H).

tive to **1** in the gas phase. Using these values, the relative binding energies decrease in the order **1** > **44** > **2** (0 vs 6.4 vs 10.2 kcal mol^{-1}).

In all cases the ligand is destabilized upon binding to the receptor due to the steric constraints imposed by the binding site. The strain energy resulting from this distortion is calculated by comparing the energy of the ligand in its bound geometry and in the gas-phase optimized geometry. Latrunculin A (**1**) and **44** are destabilized by similar amounts (15.2 and 16.8 kcal mol^{-1}, respectively), but less so than latrunculin B (**2**, 21.5 kcal mol^{-1}).

In summary, the differences in the H-bond network, in concert with the distortion energies of the ligands, offer a qualitative understanding of the changes in the biological activity for the individual compounds. Latrunculin A (**1**) and **44** both have similar H-bond network strengths and present similar ligand distortion. The hydrophobic effect, however, slightly favors **1**. Thus, we expect **1** and **44** to have similar binding abilities to the receptor. In contrast, the H-bond network is weaker for latrunculin B (**2**) and the distortion of the ligand from its optimum geometry is larger in this case. The hydrophobic contribution should slightly favor **2** over **44**, although it is still lower than for **1**. Thus, from these structural arguments we expect that the binding ability follows the order **1** ≥ **44** > **2**, which is in good agreement with the experimental results.

The role of dynamic effects in influencing the binding ability of **1** and its analogues, however, is an open question. The optimized structures of the ligands bound to actin show them to be partially buried in a hydrophobic pocket that must open in order for the ligand to bind or unbind to the receptor. This description is consistent with earlier reports of inorganic phosphates binding in a region close to the ligand-binding pocket, where it was found that significant changes in subdomain 2 of actin are required for binding the phosphate.[40] A dynamic modulation of the binding mechanism (conformation gating) has been shown previously to affect the selectivity of some enzymes.[41,42] The role that such a mechanism plays in the binding of **1** and its analogues is the focus of current work.

Conclusion

The largely catalysis-based and highly convergent total synthesis of latrunculin A (**1**) and B (**2**) outlined in the accompanying paper was diverted to the preparation of a focused library of analogues of these potent actin-binding macrolides that enjoy widespread use in chemical biology. The chosen approach allowed for structural variations of all characteristic parts of the natural leads and hence enabled the first systematic mapping of the previously largely unknown structure/activity profile of this class of bioactive natural products. Thereby it was found that the removal of the methyl branches decorating the macrocycle in **2** engenders a significant increase in potency, while streamlining the synthesis to a considerable extent. Moreover, compelling evidence is provided that the conspicuous 2-thiazolidinone ring present in all naturally occurring latrunculins is not essential for actin binding and can be replaced by an oxazolidinone moiety. Even though this engenders a slight loss in efficacy, the cytotoxicity of the corresponding products is also reduced compared to their thiazolidinone analogues. Furthermore, the inversion of the absolute configuration of the chiral center at C16 is well accommodated. Taken together, these results clearly illustrate the power of "diverted total synthesis", as none of the relevant structural variations could be achieved by derivatization of the natural leads without undue preparative efforts. Finally, the relative potency of three prototype members of this series (**1** ≥ **44** > **2**) could be rationalized by a computational analysis of their binding abilities to G-actin. This study revealed subtle differences in the hydrogen bond network engaged by these ligands as well as distortion energies induced by the protein host which offer a qualitative understanding of the experimental data.

Experimental Section

General methods: All reactions were carried out in flame-dried glassware under Ar. The solvents were purified by distillation over the drying agents indicated and were transferred under Ar: THF, Et_2O, 1,4-dioxane (Mg/anthracene), CH_2Cl_2 (P_4O_{10}), MeCN, Et_3N, pyridine (CaH_2), MeOH (Mg), DMF (Desmodur, dibutyltin dilaurate), hexane, toluene (Na/K). Flash chromatography: Merck silica gel 60 (230–400 mesh). NMR: Spectra were recorded on a Bruker DPX 300, AV 400, or DMX 600 spectrometer in the solvents indicated; chemical shifts (δ) are given in ppm relative to TMS, coupling constants (J) in Hz. The solvent signals were used as references and the chemical shifts converted to the TMS scale ($CDCl_3$: $\delta_C \equiv 77.0$ ppm; residual $CHCl_3$ in $CDCl_3$: $\delta_H \equiv 7.24$ ppm; CD_2Cl_2: $\delta_C \equiv 53.8$ ppm; residual CH_2Cl_2 in CD_2Cl_2: $\delta_H \equiv 5.32$ ppm). Where indicated, the signal assignments are unambiguous; the numbering Scheme is arbitrary and is shown in the inserts. The assignments are based upon 1D and 2D spectra recorded using the following pulse sequences from the Bruker standard pulse program library: DEPT; COSY (cosygs and cosydqtp); HSQC (invietgssi) optimized for $^1J(C,H) = 145$ Hz; HMBC (inv4gslplrnd) for correlations via $^nJ(C,H)$; HSQC-TOCSY (invietgsml) using an MLEV17 mixing time of 120 ms. IR: Nicolet FT-7199 spectrometer, wavenumbers ($\tilde{\nu}$) in cm^{-1}. MS (EI): Finnigan MAT 8200 (70 eV), ESI-MS: Finnigan MAT 95, accurate mass determinations: Bruker APEX III FT-MS (7 T magnet). Melting points: Büchi melting point apparatus B-540 (corrected). Elemental analyses: H. Kolbe, Mülheim/Ruhr. All commercially available compounds (Fluka, Lancaster, Aldrich) were used as received.

The preparation of compounds **42**–**47**, together with a compilation of their analytical and spectroscopic data, can be found in ref. [13] (Supporting Information) and is therefore not repeated herein. The bare macrocycle **52** is described in ref. [22b].

Bioassay: Murine NIH/3T3 fibroblasts (CRL-1658 from ATCC) were cultured at 37 °C and 5% CO_2 in Dulbecco's modified Eagle's medium supplemented with 4 mM L-glutamine, 4.5 g L^{-1} glucose and 10% bovine calf serum. 2×10^4 cells were seeded on coverslips in one well of a 24-well plate. After adapting and attaching over night, the cells were incubated with 1 μM, 5 μM or 10 μM of the corresponding latrunculin compound for 18 h. Before and after each fixation or staining step the cells were washed three times with TPBS (0.2% Tween20 in phosphate-buffered saline). Cells were fixed with 3.7% formalin in PBS. For blocking unspecific epitopes, fixed cells were incubated with 1% powdered milk in PBS. Actin filaments were stained for 1 h with a solution of 77 nM TRITC labeled phalloidin (P1951, Sigma) in TPBS. Cell nuclei were stained with

DAPI (2-(4-amidinophenyl)-6-indolecarbamidine dihydrochloride, D9542, Sigma). Cells were visualized and photographed with a Zeiss Axiophot fluorescence microscope.

Methyl (4*S*)-2-oxo-1,3-oxazolidine-4-carboxylate (22):[43] Triethylamine (13.4 mL, 96.3 mmol) was added at 0 °C over 5 min to a stirred suspension of serine methyl ester hydrochloride **21** (5.0 g, 32.1 mmol) in CH_2Cl_2 (75 mL). The reaction mixture was stirred for 10 min before a solution of triphosgene (3.2 g, 10.9 mmol) in CH_2Cl_2 (25 mL) was added dropwise over 2 h. The reaction was stirred for 30 min, diluted with Et_2O (75 mL) and cooled to −78 °C to precipitate all Et_3NHCl salts. The mixture was filtered and then concentrated to approx. 10 mL when it was applied carefully to a 2.5 cm depth column of silica (prepacked EtOAc) in a 100 mL sinter funnel. The solution was washed through the column with EtOAc (300 mL) and the filtrate was concentrated to give **22** as a colorless oil (4.64 g, 99 %). $[\alpha]_D^{20} = -2.0$ (*c* 0.62, EtOH); ^{1}H NMR (300 MHz, $CDCl_3$): $\delta = 3.82$ (s, 3H), 4.43 (dd, $J = 9.5$, 4.5 Hz, 1H), 4.57 (dd, $J = 8.9$, 4.5 Hz, 1H), 4.60 (d, $J = 9.5$ Hz, 1H), 6.38 (br s, 1H); ^{13}C NMR (75 MHz, $CDCl_3$): $\delta = 53.2$, 53.8, 66.8, 159.1, 170.6; IR (film): $\tilde{\nu}$ = 3296, 2959, 1732, 1480, 1438, 1399, 1366, 1213, 1115, 1056, 1007, 954, 920, 825, 766 cm^{-1}; MS (EI): *m*/*z* (%): 145 (7), 86 (100), 58 (11), 42 (55); HRMS (EI): *m*/*z*: calcd for $C_5H_7NO_4$: 145.0375; found: 145.0372.

Methyl (4*S*)-3-(4-methoxybenzyl)-2-oxo-1,3-oxazolidine-4-carboxylate (23): A solution of **22** (3.5 g, 24.1 mmol) in THF (30 mL) was slowly added at −15 °C to a slurry of NaH (0.61 g, 25.3 mmol) in THF (50 mL). The reaction was allowed to stir for 3 h before a solution of *p*-methoxybenzyl bromide (PMBBr, 8.5 g, 42 mmol) in THF (20 mL) was added dropwise. The reaction was stirred for 16 h before it was quenched with aq. sat. NH_4Cl (40 mL). The aqueous phase was extracted with *tert*-butyl methyl ether (2×40 mL), the combined organic layers were dried (Na_2SO_4) and evaporated, and the residue was purified by flash chromatography (hexane/EtOAc 3:1) to give product **23** as a white solid (3.57 g, 56 %). M.p. 65–67 °C; $[\alpha]_D^{20} = -25.0$ (*c* 0.45, EtOH); ^{1}H NMR (300 MHz, $CDCl_3$): $\delta = 3.76$ (s, 3H), 3.81 (s, 3H), 4.09 (dd, $J = 9.4$, 5.1 Hz, 1H), 4.18 (d, $J = 14.7$ Hz, 1H), 4.32 (dd, $J = 9.0$, 5.1 Hz, 1H), 4.38 (dd, $J = 9.4$, 9.0 Hz, 1H), 4.84 (d, $J = 14.7$ Hz, 1H), 6.87 (app d, $J = 8.6$ Hz, 2H), 7.19 (app d, $J = 8.6$ Hz, 2H); ^{13}C NMR (75 MHz, $CDCl_3$): $\delta = 46.8$, 52.9, 55.4, 55.9, 64.4, 114.3, 127.1, 130.0, 157.6, 159.6, 170.0; IR (film): $\tilde{\nu}$ = 2973, 2959, 1732, 1613, 1585, 1515, 1466, 1435, 1415, 1364, 1316, 1302, 1285, 1245, 1209, 1174, 1113, 1086, 1048, 1025, 1009, 980, 966, 946, 921, 870, 837, 828, 814, 756, 744, 715, 671 cm^{-1}; MS (EI): *m*/*z* (%): 265 (28), 179 (30), 162 (14), 135 (16), 134 (37), 121 (100), 78 (11); HRMS (EI): *m*/*z*: calcd for $C_{13}H_{15}NO_5$: 265.0950; found: 265.0952.

(4*S*)-*N*-Methoxy-3-(4-methoxybenzyl)-*N*-methyl-2-oxo-1,3-oxazolidine-4-carboxamide (24): Aqueous KOH (2.15 g in 35 mL of H_2O, 38 mmol) was added to a solution of **23** (3.38 g, 12.7 mmol) in 1,4-dioxane (50 mL). After 1 h the reaction was acidified with aq. HCl (2 M) and diluted with *tert*-butyl methyl ether (200 mL). The aqueous layer was extracted with *tert*-butyl methyl ether (2×100 mL), the combined organic phases were washed with brine, dried (Na_2SO_4) and concentrated to an oil. Repeated treatment of the oil with toluene/CH_2Cl_2 2:1 followed by re-evaporation resulted in removal of residual water and isolation of (4*S*)-3-(4-methoxybenzyl)-2-oxo-1,3-oxazolidine-4-carboxylic acid as a white solid (3.1 g, 97 %). M.p. 116–118 °C; $[\alpha]_D^{20} = -28.1$ (*c* 1.0, EtOH); ^{1}H NMR (300 MHz, [D]$_6$DMSO): $\delta = 3.76$ (s, 3H), 4.09 (d, $J = 15.1$ Hz, 1H), 4.14 (dd, $J = 9.4$, 4.4 Hz, 1H), 4.29 (dd, $J = 8.9$, 4.4 Hz, 1H), 4.47 (t, $J = 9.4$ Hz, 1H), 4.62 (d, $J = 15.1$ Hz, 1H), 6.93 (app d, $J = 8.7$ Hz, 2H), 7.21 (app d, $J = 8.7$ Hz, 2H); ^{13}C NMR (75 MHz, $CDCl_3$): $\delta = 45.8$, 55.1, 55.8, 64.5, 114.0, 127.7, 129.4, 157.3, 158.8, 171.3; IR (film): $\tilde{\nu}$ = 3440, 2958, 2934, 2838, 2722, 2611, 2509, 1743, 1689, 1612, 1587, 1514, 1470, 1444, 1419, 1365, 1294, 1268, 1248, 1197, 1179, 1116, 1101, 1030, 971, 834, 813, 762, 746, 677 cm^{-1}; MS (EI): *m*/*z* (%): 251 (58), 206 (5), 179 (81), 162 (15), 134 (94), 121 (100), 78 (16), 77 (15); HRMS (EI): *m*/*z*: calcd for $C_{12}H_{13}NO_5$: 251.0793; found: 251.0794.

To a solution of this acid (1.0 g, 4 mmol) in CH_2Cl_2 (10 mL) was added (benzotriazol-1-yloxy) tris-(dimethylamino)-phosphonium hexafluorophosphate (BOP, 1.8 g, 4 mmol) shortly followed by Et_3N (0.58 mL, 4.2 mmol). The reaction was stirred for 10 min before *N*,*O*-dimethylhydroxylamine hydrochloride (0.43 g, 4.4 mmol) was added along with another portion of Et_3N (0.58 mL, 4.2 mmol). The mixture was stirred overnight and was quenched with sat. aq. NH_4Cl, the aqueous phase was extracted with CH_2Cl_2 (3×20 mL) and the combined organics were dried (Na_2SO_4) and evaporated. The residue was purified by flash chromatography (hexane/EtOAc 1:2) to give **24** as a light yellow oil (1.16 g, 99 %). $[\alpha]_D^{20} = -4.5$ (*c* 0.37, EtOH); ^{1}H NMR (400 MHz, [D]$_6$DMSO): $\delta = 3.12$ (s, 3H), 3.51 (s, 3H), 3.76 (s, 3H), 4.01 (d, $J = 14.9$ Hz, 1H), 4.19 (dd, $J = 6.6$, 2.2 Hz, 1H), 4.47–4.55 (m, 2H), 4.62 (d, $J = 14.9$ Hz, 1H), 6.93 (app d, $J = 8.7$ Hz, 2H), 7.21 (app d, $J = 8.7$ Hz, 2H); ^{13}C NMR (100 MHz, $CDCl_3$): $\delta = 32.0$, 45.7, 53.9, 54.9, 61.2, 64.2, 113.9, 127.6, 129.4, 157.6, 158.7, 169.0; IR (film): $\tilde{\nu}$ = 3478, 2941, 2839, 1755, 1673, 1612, 1586, 1514, 1443, 1419, 1376, 1323, 1304, 1249, 1210, 1178, 1116, 1083, 1034, 997, 960, 846, 762, 559 cm^{-1}; MS (EI): *m*/*z* (%): 294 (7), 263 (23), 162 (6), 121 (100), 78 (6), 55 (7); HRMS (ESI): *m*/*z*: calcd for $C_{14}H_{18}N_2O_5$+Na: 317.1113; found: 317.1112 [M^++Na].

(4*S*)-4-Acetyl-3-(4-methoxybenzyl)-1,3-oxazolidin-2-one (6): MeMgBr (2.9 mL, 3 M in Et_2O, 8.6 mmol) was added at −40 °C to a solution of compound **24** (2.4 g, 8.2 mmol) in THF (25 mL). The reaction was stirred at −40 °C for 1 h and then allowed to warm to −20 °C for 2 h. The reaction was quenched with sat. aq. NH_4Cl, the organic phase was separated and the aqueous layer extracted with EtOAc (3×20 mL), the combined organic phases were dried (Na_2SO_4) and evaporated, and the residue was purified by flash chromatography (hexane/EtOAc 1:1) to give ketone **6** as a white solid (1.95 g, 96 %). Chiral LC/MS showed that the product had an *ee* of 77.3 %. The material was recrystallized from *tert*-butyl methyl ether to give white crystals (1.66 g, 82 %, 97.2 % *ee*). M.p. 65–67 °C; $[\alpha]_D^{20} = -26.5$ (*c* 1.0, $CHCl_3$); ^{1}H NMR (400 MHz, $CDCl_3$): $\delta = 2.07$ (s, 3H), 3.81 (s, 3H), 4.06 (dd, $J = 9.8$, 5.6 Hz, 1H), 4.11 (d, $J = 14.6$ Hz, 1H), 4.13 (dd, $J = 8.9$, 5.6 Hz, 1H), 4.43 (dd, $J = 9.8$, 8.9 Hz, 1H), 4.80 (d, $J = 14.6$ Hz, 1H), 6.87 (app d, $J = 8.7$ Hz, 2H), 7.16 (app d, $J = 8.7$ Hz, 2H); ^{13}C NMR (75 MHz, $CDCl_3$): $\delta = 25.9$, 47.1, 55.4, 62.4, 63.5, 114.4, 126.9, 130.1, 157.8, 159.7, 204.3; IR (film): $\tilde{\nu}$ = 3002, 2935, 2838, 1756, 1725, 1612, 1586, 1514, 1443, 1412, 1362, 1304, 1248, 1207, 1176, 1115, 1077, 1038, 846, 754 cm^{-1}; MS (EI): *m*/*z* (%): 249 (6), 206 (9), 121 (100), 91 (3), 78 (5), 77 (4); HRMS (ESI): *m*/*z*: calcd for $C_{13}H_{15}NO_4$+Na: 272.0898; found: 272.0895 [M^++Na].

Ethyl (*Z*)-3-chloro-2-propenoate (26):[44] A mixture of ethyl propiolate **25** (2.0 g, 20.4 mmol, 2.04 mL), dry lithium chloride (0.95 g) and acetic acid (1.3 mL) in MeCN (25 mL) was refluxed for 18 h. The reaction was allowed to cool and water added (100 mL). Solid K_2CO_3 was added until no further CO_2 evolution occurred. The organic layer was separated and the aqueous phase extracted with *tert*-butyl methyl ether (3×100 mL). The combined organic extracts were dried (Na_2SO_4) and evaporated. Purification of the residue by flash chromatography gave **26** as a colorless liquid (1.66 g, 60 %). ^{1}H NMR (300 MHz, $CDCl_3$): $\delta = 1.32$ (t, $J = 7.1$ Hz, 3H), 4.25 (q, $J = 7.1$ Hz, 2H), 6.20 (d, $J = 8.2$ Hz, 1H), 6.71 (d, $J = 8.2$ Hz, 1H); ^{13}C NMR (100 MHz, $CDCl_3$): $\delta = 163.4$, 132.3, 121.5, 60.7, 14.2; MS (EI): *m*/*z* (%): 106 (9), 99 (42), 91 (34), 89 (100), 61 (20), 45 (14); HRMS (CI, isobutane): *m*/*z*: calcd for $C_5H_7ClO_2$: 135.0212; found: 135.0210 [M^++H].

Ethyl (*Z*)-2-octen-6-ynoate (28): Magnesium turnings (433 mg, 17.8 mmol) were stirred with I_2 for 1 h. THF (2 mL) was added and a solution of 5-pentynyl bromide (2.3 g, 16.0 mmol) in THF (17 mL) was added dropwise to maintain gentle reflux. After complete addition, the mixture was refluxed for 1.5 h before allowing to cool. The solution of the Grignard reagent **27** thus formed was quickly added in one portion to a solution of chloride **26** (1.0 g, 7.4 mmol) and [Fe(acac)$_3$] (565 mg, 10 mol %) in THF (15 mL) at −30 °C. After 10 min the reaction was allowed to warm to room temperature before quenching with sat. aq. NH_4Cl. The organic layers were separated and the aqueous phase was extracted with *tert*-butyl methyl ether. The combined organic layers were dried (Na_2SO_4), the solvent was evaporated and the residue purified by flash chromatography (hexane/EtOAc 20:1) to give **28** as a volatile light yellow oil (964 mg, 78 %). ^{1}H NMR (300 MHz, $CDCl_3$): $\delta = 1.28$ (t, $J = 7.1$ Hz, 3H), 1.77 (t, $J = 2.5$ Hz, 3H), 2.27 (m, 2H), 2.82 (dd, $J = 7.2$, 1.7 Hz, 2H), 4.16 (q, $J = 7.1$ Hz, 2H), 5.81 (ddd, $J = 1.7$, 1.7, 11.4 Hz, 1H), 6.32 (dd, $J = 7.2$, 11.4 Hz, 1H); ^{13}C NMR (100 MHz, $CDCl_3$): $\delta = 3.5$, 14.3, 18.4, 28.4, 59.9, 76.4, 78.0, 120.7, 148.3, 166.3; IR (film): $\tilde{\nu}$ = 2981, 2920,

1716, 1646, 1445, 1414, 1388, 1332, 1283, 1216, 1188, 1163, 1096, 1030, 821 cm^{-1}; HRMS (CI, isobutane): *m/z*: calcd for $C_{10}H_{15}O_2$: 167.1072; found: 167.1073 [M^++H].

(*Z*)-2-Octen-6-ynoic acid (9): Aq. NaOH (1 M, 12.4 mL, 12.4 mmol) was added to a stirred solution of ester **28** (773 mg, 4.65 mmol) in MeOH (10 mL). The reaction was allowed to stir overnight before removal of the methanol under vacuum. The aqueous layer was washed with *tert*-butyl methyl ether and the organic phases were discarded. The aqueous layer was acidified to pH 1 with aq. HCl (2 M) and extracted with CH_2Cl_2 (3×20 mL). The combined organic phases were dried (Na_2SO_4) and evaporated and the residue was purified by Kugelrohr distillation to give **9** as a colorless liquid (571 mg, 74%). ^{1}H NMR (300 MHz, $CDCl_3$): δ = 1.77 (t, *J* = 2.5 Hz, 3H), 2.23–2.32 (m, 2H), 2.82 (dd, *J* = 7.1, 1.7 Hz, 2H), 5.84 (ddd, *J* = 11.5, 1.6, 1.6 Hz, 1H), 6.44 (ddd, *J* = 11.5, 7.1, 7.1 Hz, 1H), 11.5 (br s, 1H); ^{13}C NMR (100 MHz, $CDCl_3$): δ = 3.5, 18.4, 28.7, 76.7, 77.7, 120.0, 151.3, 171.8; IR (film): $\tilde{\nu}$ = 2970, 2921, 1737, 1695, 1432, 1366, 1287, 1231, 1217, 1204, 1110, 924, 826, 722 cm^{-1}; HRMS (CI, isobutane): *m/z*: calcd for $C_8H_{11}O_2$: 139.0759; found: 139.0760 [M^++H].

(1*R*)-1-Allyl-5-heptynyl *tert*-butyl(dimethyl)silyl ether (31): A solution of 5-heptynal **29** (1.4 g, 12.7 mmol) in diethyl ether (20 mL) was added at −100 °C to a stirred solution of (−)-Ipc$_2$B(allyl)[45] (25.4 mL, 0.5 M in Et_2O, 12.7 mmol). The reaction was allowed to stir for 1 h at −100 °C and then quenched with MeOH (1 mL). The solvent was removed under vacuum at 0 °C and the residue dissolved in MeOH (26 mL). 8-Hydroxyquinoline (2.3 g) was added and the reaction stirred overnight. The yellow precipitate formed was filtered off and the filtrate evaporated to dryness. Purification of the residue by flash chromatography (hexane/EtOAc 40:1) gave slightly impure alcohol **30** as a light brown oil (1.93 g; 91% *ee*, GC) which was directly used in the next step.

The crude material was dissolved in DMF (20 mL) followed by the addition of TBSCl (2.4 g, 15.88 mmol) and imidazole (1.7 g, 25.4 mmol). The reaction was stirred overnight before it was diluted with hexane (250 mL). The solution was successively washed with 5% aq. HCl, sat. aq. $NaHCO_3$, water and brine followed by drying (Na_2SO_4) of the organic phase and evaporation of the solvent. The residue was purified by flash chromatography (hexane/EtOAc 40:1) to give product **31** as a colorless oil (2.05 g, 68% over both steps). $[\alpha]_D^{20}$ = +9 (*c* 0.07, $CHCl_3$); ^{1}H NMR (300 MHz, $CDCl_3$): δ = 0.06 (s, 6H), 0.89 (s, 9H), 1.53 (m, 4H), 1.78 (t, *J* = 2.5 Hz, 3H), 2.12 (m, 2H), 2.22 (ddd, *J* = 7.1, 5.9, 1.2 Hz, 2H), 3.72 (m, 1H), 5.02 (s, 1H), 5.06 (m, 1H), 5.82 (m, 1H); ^{13}C NMR (75 MHz, $CDCl_3$): δ = −4.4, −4.3, 3.6, 18.2, 18.9, 24.9, 26.0, 36.0, 41.9, 71.8, 75.7, 79.3, 116.8, 135.4; IR (film): $\tilde{\nu}$ = 2952, 2929, 2857, 1472, 1462, 1435, 1361, 1254, 1088, 1005, 938, 911, 880, 834, 808, 772, 665 cm^{-1}; MS (EI): *m/z* (%): 225 (4), 209 (5), 185 (3), 133 (14), 99, (22), 93, (44), 75 (100), 73 (67); HRMS (CI, isobutane): *m/z*: calcd for $C_{16}H_{30}OSi$: 267.2144; found: 267.2141 [M^++H].

(3*R*)-3-{[*tert*-Butyl(dimethyl)silyl]oxy}-7-nonynal (14): A stirred solution of compound **31** (2.01 g, 8.43 mmol) and trace amounts of Sudan Red 7B (enough to give red color) in MeOH (100 mL) at −78 °C was treated with ozone until the red color disappeared. Argon was bubbled through the solution for 15 min before PPh_3 (3.3 g, 1.5 equiv) was added and the reaction left to stir overnight. The solvent was evaporated and the residue purified by flash chromatography (hexane → hexane/EtOAc 20:1) to give aldehyde **14** as a colorless oil (1.51 g, 67%). $[\alpha]_D^{20}$ = −7.8 (*c* 0.7, $CHCl_3$); ^{1}H NMR (300 MHz, $CDCl_3$): δ = 0.07 (s, 3H), 0.09 (s, 3H), 0.88 (s, 9H), 1.46–1.70 (m, 6H), 1.78 (t, *J* = 2.5 Hz, 3H), 2.15 (dddd, *J* = 9.2, 5.1, 2.5, 2.4 Hz, 2H), 2.52 (dd, *J* = 2.4, 1.5 Hz, 1H), 2.54 (t, *J* = 2.4 Hz, 1H), 4.23 (tt, *J* = 5.7 Hz, 1H), 9.82 (t, *J* = 2.5 Hz, 1H); ^{13}C NMR (75 MHz, $CDCl_3$): δ = −4.3, −4.0, 18.4, 19.1, 24.9, 26.1, 37.2, 51.1, 68.2, 76.4, 77.6, 79.0, 202.6; IR (film): $\tilde{\nu}$ = 2954, 2930, 2858, 2712, 1713, 1472, 1463, 1436, 1409, 1389, 1376, 1361, 1295, 1256, 1217, 1098, 1027, 1006, 939, 837, 811, 776, 680, 665 cm^{-1}; MS (EI): *m/z* (%): 211 (50), 169 (41), 167 (32), 157 (13), 129 (10), 119 (19), 101 (100), 93 (56), 75 (64), 59 (39); HRMS (CI, isobutane): *m/z*: calcd for $C_{15}H_{28}O_2Si$: 269.1936; found: 269.1933 [M^++H].

Titanium aldol reaction: $TiCl_4$ (1 M in CH_2Cl_2, 1.35 mL, 1.35 mmol) was added at −78 °C to a solution of ketone **7** (311 mg, 1.25 mmol) in CH_2Cl_2 (5 mL). The reaction was allowed to stir for 20 min before (iPr)$_2$NEt (1 M in CH_2Cl_2, 1.7 mL, 1.7 mmol) was introduced. After stirring for 2 h at −78 °C, the reaction was warmed to 0 °C and allowed to stir for 3 h. The reaction was cooled to −78 °C and a solution of aldehyde **14** (250 mg, 1.04 mmol) in CH_2Cl_2 (5 mL) was added dropwise. After stirring for 3 h at −78 °C, the reaction was quenched with aq. NH_4Cl and the mixture allowed to warm to room temperature before water was added to dissolve the salts. The organic layer was separated and the aqueous phase extracted with CH_2Cl_2 (3×20 mL).

The combined organic layers were washed with aq. $NaHCO_3$ and brine, dried (Na_2SO_4) and concentrated. The residue was purified by flash chromatography (hexane/EtOAc 2:1) to give the product in form of two diastereomers that were separable by chromatography (hexane/EtOAc 3:1).

Major isomer 32: Colorless oil (163 mg, 30%); $[\alpha]_D^{20}$ = −4.4 (*c* 0.73, $CHCl_3$); ^{1}H NMR (400 MHz, $CDCl_3$): δ = 0.09 (d, *J* = 4.6 Hz, 6H), 0.87 (s, 9H), 1.37–1.61 (m, 6H), 1.74 (t, *J* = 2.5 Hz, 3H), 2.07–2.14 (m, 2H), 2.21 (dd, *J* = 15.3, 3.7 Hz, 1H), 2.51 (dd, *J* = 15.3, 8.7 Hz, 1H), 3.51 (br s, 1H), 3.77 (s, 3H), 3.90–3.97 (m, 1H), 4.02 (d, *J* = 14.7 Hz, 1H), 4.08–4.15 (m, 1H), 4.19 (m, 2H), 4.35 (m, 1H), 4.73 (d, *J* = 14.7 Hz, 1H), 6.81 (app d, *J* = 8.6 Hz, 2H), 7.13 (app d, *J* = 8.6 Hz, 2H); ^{13}C NMR (100 MHz, $CDCl_3$): δ = −4.8, −4.1, 3.3, 17.8, 18.6, 23.9, 25.7, 36.6, 42.4, 46.6, 46.8, 55.1, 62.4, 63.0, 67.7, 72.3, 75.9, 78.5, 114.1, 127.1, 130.0, 157.8, 159.5, 205.7; IR (film): $\tilde{\nu}$ = 3462, 2941, 2929, 2857, 1747, 1612, 1514, 1412, 1371, 1303, 1248, 1176, 1075, 1032, 835, 809, 774, 731, 663 cm^{-1}; MS (EI): *m/z* (%): 460 (1), 442 (6), 211 (4), 206 (3), 169 (3), 167 (3), 122 (8), 121 (100), 101 (9), 93 (7), 91 (2), 75 (9), 73 (7), 59 (4); HRMS (ESI): *m/z*: calcd for $C_{28}H_{43}NO_6Si$: 518.2937; found: 518.2935 [M^++H].

Minor isomer 33: White solid (147 mg, 28%); m.p. 77–79 °C; $[\alpha]_D^{20}$ = +33.6 (*c* 0.78, $CHCl_3$); ^{1}H NMR (400 MHz, $CDCl_3$): δ = 0.09 (s, 6H), 0.88 (s, 9H), 1.45 (m, 2H), 1.50 (ddd, *J* = 14.3, 5.2, 2.2 Hz, 1H), 1.58–1.73 (m, 3H), 1.76 (t, *J* = 2.5 Hz, 3H), 2.10–2.16 (m, 2H), 2.31 (dd, *J* = 15.9, 3.7 Hz, 1H), 2.49 (dd, *J* = 15.9, 8.5 Hz, 1H), 3.63 (br s, 1H), 3.78 (s, 3H), 3.95–4.01 (m, 1H), 4.04 (d, *J* = 14.7 Hz, 1H), 4.11 (dd, *J* = 9.6, 5.6 Hz, 1H), 4.19 (dd, *J* = 8.9, 5.6 Hz, 1H), 4.34–4.42 (m, 2H), 4.83 (d, *J* = 14.7 Hz, 1H), 6.84 (app d, *J* = 8.6 Hz, 2H), 7.12 (app d, *J* = 8.6 Hz, 2H); ^{13}C NMR (100 MHz, $CDCl_3$): δ = −4.8, −4.6, 3.4, 17.9, 18.7, 25.0, 25.7, 35.2, 41.1, 46.7, 47.2, 55.2, 62.0, 63.3, 64.9, 70.8, 76.0, 78.6, 114.2, 127.0, 110.0, 157.9, 159.5, 205.9; IR (KBr): $\tilde{\nu}$ = 3415, 2952, 2932, 2857, 1723, 1613, 1516, 1451, 1433, 1347, 1307, 1256, 1225, 1185, 1102, 1069, 1032, 1018, 941, 930, 838, 823, 808, 767, 753, 740, 726, 660 cm^{-1}; MS (EI): *m/z* (%): 499 (0.8), 442 (11), 249 (6), 206 (8), 169 (8), 121 (100), 101 (12); HRMS (ESI): *m/z*: calcd for $C_{28}H_{43}NO_6Si$+Na: 540.2757; found: 540.2751 [M^++Na].

(4*R*)-4-[(2*R*,4*S*,6*R*)-6-(4-Hexynyl)-4-hydroxy-2-methoxytetrahydro-2*H*-pyran-2-yl]-3-(4-methoxybenzyl)-1,3-oxazolidin-2-one (34): Aq. HCl (1 M, 1.6 mL) was added to a stirred solution of aldol **33** (315 mg, 0.61 mmol) in THF (12 mL). The reaction was stirred overnight and then quenched with aq. $NaHCO_3$, the aqueous layer was extracted with CH_2Cl_2 (4×20 mL), the combined organic phases were washed with sat. aq. NaCl and dried (Na_2SO_4). After evaporation of the solvent the residue was purified by flash chromatography (hexane/EtOAc 1:1) to give the corresponding hemiacetal which was used without delay in the next reaction. A catalytic amount of camphorsulfonic acid (CSA) was added to a solution of the crude hemiacetal in methanol (4 mL). The reaction was stirred overnight before quenching with sat. aq. $NaHCO_3$. The aqueous phase was extracted with CH_2Cl_2 (3×5 mL), the combined organic layers were washed with brine, dried (Na_2SO_4) and evaporated. The residue was purified by flash chromatography (hexane/EtOAc 2:1) to give glycoside **34** (77 mg, 92%) as a colorless oil. $[\alpha]_D^{20}$ = +30.6 (*c* 0.41, $CHCl_3$); ^{1}H NMR (400 MHz, $CDCl_3$): δ = 1.38–1.50 (m, 2H), 1.51–1.62 (m, 3H), 1.65 (dd, *J* = 14.4, 3.7 Hz, 1H), 1.73 (t, *J* = 2.5 Hz, 3H), 1.77–1.88 (m, 2H), 2.07–2.13 (m, 2H), 3.07 (s, 3H), 3.64 (br s, 1H), 3.78 (s, 3H), 3.81 (dd, *J* = 9.3, 4.7 Hz, 1H), 3.83–3.89 (m, 1H), 4.12–4.26 (m, 4H), 4.94 (d, *J* = 15.2 Hz, 1H), 6.86 (app d, *J* = 8.5 Hz, 2H), 7.17 (app d, *J* = 8.5 Hz, 2H); ^{13}C NMR (100 MHz, $CDCl_3$): δ = 3.4, 18.8, 24.9, 32.5, 34.6, 37.4, 46.2, 47.9, 53.8,

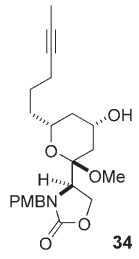

34

55.3, 63.6, 64.2, 65.2, 75.9, 78.5, 102.1, 114.2, 128.1, 128.9, 158.9, 159.3; IR (film): $\tilde{\nu}$ = 3520, 2942, 2838, 1745, 1612, 1585, 1513, 1439, 1410, 1366, 1303, 1287, 1229, 1175, 1103, 1080, 1026, 957, 886, 819, 766, 751, 735, 717, 675 cm^{-1}; MS (EI): *m/z* (%): 417 (0.3), 211 (53), 193 (8), 179 (19), 161 (15), 151 (9), 138 (7), 137 (80), 121 (100), 119 (56), 111 (17), 109 (10), 95 (14), 93 (10), 91 (13); HRMS (ESI): *m/z*: calcd for $C_{23}H_{31}NO_6$+Na: 440.2049; found: 440.2046 [M^++Na].

(4*R*)-4-[(2*R*,4*R*,6*R*)-6-(4-hexynyl)-4-hydroxy-2-methoxytetrahydro-2*H*-pyran-2-yl]-3-(4-methoxybenzyl)-1,3-oxazolidin-2-one (35): Prepared analogously from aldol **32**; colorless oil (58 mg, 88%); $[\alpha]_D^{20}$ = +30.0 (*c* 0.41, $CHCl_3$); ^{1}H NMR (400 MHz, $CDCl_3$): δ = 1.20 (m, 1H), 1.27–1.35 (m, 1H), 1.39–1.49 (m, 1H), 1.52–1.61 (m, 3H), 1.74 (t, *J* = 2.5 Hz, 3H), 1.92–2.03 (m, 2H), 2.07–2.13 (m, 2H), 2.53 (brs, 1H), 2.97 (s, 3H), 3.47–3.55 (m, 1H), 3.79 (s, 3H), 3.85 (dd, *J* = 7.3, 6.8 Hz, 1H), 4.03 (dddd, *J* = 10.4, 10.3, 4.3, 4.2 Hz, 1H), 4.18–4.26 (m, 3H), 4.92 (d, *J* = 15.3 Hz, 1H), 6.86 (app d, *J* = 8.6 Hz, 2H), 7.18 (app d, *J* = 8.6 Hz, 2H); ^{13}C NMR (100 MHz, $CDCl_3$): δ = 3.4, 18.8, 24.9, 34.7, 36.9, 40.1, 46.1, 47.7, 53.5, 55.3, 64.3, 69.8, 75.9, 78.6, 101.8, 114.2, 128.4, 128.9, 159.2; IR (film): $\tilde{\nu}$ = 3442, 2970, 2946, 1739, 1612, 1513, 1440, 1413, 1365, 1229, 1217, 1175, 1141, 1113, 1082, 1022, 963, 819, 751 cm^{-1}; MS (EI): *m/z* (%): 417 (0.5), 211 (51), 193 (7), 179 (12), 161 (21), 151 (7), 137 (64), 133 (43), 121 (100), 119 (60), 111 (18), 109 (13), 103 (15), 95 (34), 93 (11), 91 (15), 71 (11); HRMS (ESI): *m/z*: calcd for $C_{23}H_{31}NO_6$+Na: 440.2049; found: 440.2046 [M^++Na].

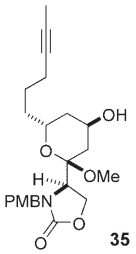

35

Ester 36: Triflic anhydride (27 μL, 0.16 mmol) was added to a cooled (−78 °C) solution of compound **34** (56.6 mg, 0.136 mmol) and pyridine (22 μL, 0.27 mmol) in CH_2Cl_2 (5 mL). The mixture was warmed to −45 °C and stirred at that temperature for 4 h. For work up, the reaction was quenched with aq. $KHSO_4$ (15 mL, 10% *w/w*) and ice, the aqueous layer was repeatedly extracted with CH_2Cl_2, the combined organic phases were dried over Na_2SO_4, filtered and evaporated. The resulting triflate was dissolved in THF (7.5 mL) and added to a cooled solution (0 °C) of NaH (15.6 mg, 0.390 mmol) and acid **9** (59.3 mmol, 0.429 mmol) in THF (5 mL) [which had been stirred for 30 min at ambient temperature and for additional 30 min at reflux temperature prior to use]. The resulting mixture was stirred for 15 h at ambient temperature before it was poured into sat. aq. $NaHCO_3$. The aqueous layer was extracted with EtOAc (3× 10 mL), the combined organic phases were dried (Na_2SO_4) and evaporated, and the residue was purified by flash chromatography (hexanes/EtOAc 2:1) to afford diyne **36** as a colorless oil (51.5 mg, 70%). $[\alpha]_D^{20}$ = +57.7 (*c* 1.02, $CHCl_3$); ^{1}H NMR (400 MHz, $CDCl_3$): δ = 7.19 (d, *J* = 8.6 Hz, 2H), 7.00 (dt, *J* = 15.7, 6.6 Hz, 1H), 6.85 (d, *J* = 8.6 Hz, 2H), 5.88 (dt, *J* = 15.7, 1.5 Hz, 1H), 5.19 (m, 1H), 4.88 (d, *J* = 15.2 Hz, 1H), 4.25–4.08 (m, 2H), 4.21 (d, *J* = 15.2 Hz, 1H), 3.91–3.83 (m, 1H), 3.83–3.77 (m, 1H), 3.79 (s, 3H), 3.07 (s, 3H), 2.44–2.37 (m, 2H), 2.35–2.27 (m, 2H), 2.15–2.08 (m, 2H), 1.96 (dt, *J* = 15.2, 1.9 Hz, 1H), 1.86–1.79 (m, 1H), 1.78 (t, *J* = 2.5 Hz, 3H), 1.74 (t, *J* = 2.5 Hz, 3H), 1.64 (dd, *J* = 15.2, 4.3 Hz, 2H), 1.57–1.41 (m, 4H); ^{13}C NMR (100 MHz, $CDCl_3$): δ = 165.7 (C), 159.2 (C), 159.0 (C), 147.4 (CH), 129.0 (CH), 128.5 (C), 122.5 (CH), 114.1 (CH), 99.9 (C), 78.5 (C), 77.5 (C), 76.6 (C), 75.9 (C), 66.6 (CH), 65.3 (CH), 64.2 (CH_2), 55.2 (CH_3), 54.2 (CH), 47.8 (CH_3), 46.2 (CH_2), 34.6 (CH_2), 34.2 (CH_2), 31.7 (CH_2), 30.7 (CH_2), 24.9 (CH_2), 18.8 (CH_2), 17.9 (CH_2), 3.4 (CH_3), 3.4 (CH_3); IR (film): $\tilde{\nu}$ = 2920, 1749, 1709, 1513, 1030 cm^{-1}; HRMS (ESI): *m/z*: calcd for $C_{31}H_{39}NO_7$+Na: 560.2624; found: 560.2621 [M^++Na].

Cycloalkyne 38: CH_2Cl_2 (245 μL, 3.81 mmol) was added to a solution of complex **40** (16 mg, 0.026 mmol)[22] in degassed toluene (2 mL). After stirring for 15 min, the resulting mixture was added to a solution of diyne **36** (51.5 mg, 0.096 mmol) in toluene (48 mL) and the resulting suspension was stirred at 80 °C for 15 h. The mixture was then allowed to cool to ambient temperature, filtered through a pad of silica, and the filtrate was evaporated. Purification of the residue by flash chromatography (hexanes/EtOAc 2:1) afforded cycloalkyne **38** as a colorless oil (33.1 mg, 71%). $[\alpha]_D^{20}$ = +46.2 (*c* 1.66, CH_2Cl_2); ^{1}H NMR (300 MHz, $CDCl_3$): δ = 7.20 (d, *J* = 8.3 Hz, 2H), 6.86 (d, *J* = 8.7 Hz, 2H), 6.27–6.15 (m, 1H), 5.81 (d, *J* = 11.7 Hz, 1H), 5.35–5.26 (m, 1H), 4.95–4.82 (m, 2H), 4.30–4.15 (m, 3H), 3.87 (dd, *J* = 9.2, 4.7 Hz, 1H), 3.79 (s, 3H), 3.50–3.35 (m, 1H), 3.14 (s, 3H), 2.51–2.35 (m, 2H), 2.27–2.16 (m, 2H), 2.03 (d, *J* = 14.7 Hz, 2H), 1.77–1.61 (m, 4H), 1.59–1.33 (m, 3H); ^{13}C NMR (75 MHz, $CDCl_3$): δ = 166.0, 159.2, 159.0, 146.1, 129.0, 128.5, 122.8, 114.1, 100.2, 81.6, 80.9, 66.8, 64.9, 64.3, 55.3, 54.0, 48.0, 46.2, 35.9, 34.1, 30.7, 28.4, 22.2, 19.6, 19.0; IR (film): $\tilde{\nu}$ = 2936, 1750, 1701, 1513 cm^{-1}; HRMS (ESI): *m/z*: calcd for $C_{27}H_{33}NO_7$+Na: 506.2155; found: 506.2159 [M^++Na].

Compound 39: Commercial Lindlar catalyst (15 mg) was added to a solution of cycloalkyne **38** (9.1 mg, 18.8 μmol) in CH_2Cl_2 (2 mL) and the resulting mixture was stirred vigorously under a hydrogen atmosphere (1 atm) overnight. For work up, the mixture was filtered through Celite and the filtrate was evaporated to give analytically pure (+)-(*R*)-3-(4-methoxybenzyl)-4-((1*R*,4*Z*,8*Z*,13*R*,15*R*)-15-methoxy-3-oxo-2,14-dioxa-bicyclo-[11.3.1]heptadeca-4,8-dien-15-yl)oxazolidin-2-one as a pale yellow oil (9.1 mg, quant.). $[\alpha]_D^{20}$ = +53.3 (*c* 1.09, CH_2Cl_2); ^{1}H NMR (400 MHz, $CDCl_3$): δ = 7.20 (d, *J* = 8.3 Hz, 2H), 6.86 (d, *J* = 8.7 Hz, 2H), 6.27–6.15 (m, 1H), 5.81 (d, *J* = 11.7 Hz, 1H), 5.35–5.26 (m, 1H), 4.95–4.82 (m, 2H), 4.30–4.15 (m, 3H), 3.87 (dd, *J* = 9.2, 4.7 Hz, 1H), 3.79 (s, 3H), 3.50–3.35 (m, 1H), 3.14 (s, 3H), 2.51–2.35 (m, 2H), 2.27–2.16 (m, 2H), 2.03 (d, *J* = 14.7 Hz, 2H), 1.77–1.61 (m, 4H), 1.59–1.33 (m, 3H); ^{13}C NMR (75 MHz, $CDCl_3$): δ = 166.0 (C), 159.2 (C), 159.0 (C), 145.5 (CH), 129.5 (CH), 129.0 (CH), 128.5 (C), 122.0 (CH), 114.1 (CH), 100.4 (C), 66.9 (CH), 64.2 (CH_2), 62.9 (CH), 55.3 (CH), 54.3 (CH_3), 47.9 (CH_3), 46.2 (CH_2), 34.1 (CH_2), 30.8 (CH_2), 30.8 (CH_2), 30.2 (CH_2), 27.3 (CH_2), 23.7 (CH_2), 21.8 (CH_2); IR (film): $\tilde{\nu}$ = 2935, 1753, 1707, 1513 cm^{-1}; HRMS (ESI): *m/z*: calcd for $C_{27}H_{35}NO_7$ + Na: 508.2311; found: 508.2308 [M^++Na].

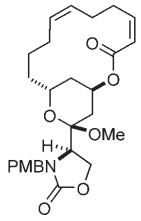

CAN (26 mg, 0.047 mmol) was added to a vigorously stirred suspension of the cycloalkene prepared above (9.1 mg, 18.7 μmol) in MeCN/water 2:1 (0.6 mL). After 20 min the mixture became homogeneous and stirring was continued for additional 21 h. The solution was extracted with CH_2Cl_2 (3×2 mL), the combined organic layers were dried (Na_2SO_4) and evaporated, and the residue was purified by flash chromatography (hexane/EtOAc 1:1) to give product **39** as a colorless oil (6.1 mg, 93%). $[\alpha]_D^{20}$ = +58.1 (*c* 1.1, $CHCl_3$); ^{1}H NMR (400 MHz, CD_2Cl_2): δ = 8.51 (s, 1H), 6.28–6.20 (m, 1H), 5.75 (d, *J* = 11.6 Hz, 1H), 5.51 (dd, *J* = 6.1, 2.0 Hz, 1H), 5.42–5.33 (m, 1H), 5.31–5.20 (m, 1H), 4.36 (t, *J* = 9.0 Hz, 1H), 4.34–4.27 (m, 1H), 4.24 (dd, *J* = 9.1, 6.1 Hz, 1H), 3.98–3.84 (m, 2H), 3.79 (ddd, *J* = 9.0, 5.9, 1.3 Hz, 1H), 3.33 (d, *J* = 1.0 Hz, 1H), 2.51–1.20 (m, 12H); ^{13}C NMR (100 MHz, CD_2Cl_2): δ = 165.9 (C), 159.7 (C), 145.6 (CH), 129.8 (CH), 129.8 (CH), 121.8 (CH), 96.4 (C), 68.3 (CH), 66.1 (CH_2), 62.5 (CH), 60.6 (CH), 35.4 (CH_2), 32.6 (CH_2), 31.5 (CH_2), 31.0 (CH_2), 27.6 (CH_2), 24.2 (CH_2), 22.4 (CH_2); IR (film): $\tilde{\nu}$ = 3337, 2924, 2858, 1747, 1706 cm^{-1}.

Compound 48: Cerium ammonium nitrate (CAN, 26 mg, 0.047 mmol) was added to a vigorously stirred suspension of cycloalkyne **53** (10 mg, 0.019 mmol)[11,14a] in MeCN/water 2:1 (0.5 mL). After 20 min the mixture became homogeneous and stirring was continued for additional 4 h. The solution was extracted with CH_2Cl_2 (3×2 mL), the combined organic layers were dried (Na_2SO_4) and the solvent was evaporated. Purification by flash chromatography (EtOAc/hexane 1:2) afforded derivative **48** as a pale yellow oil (5 mg, 80%). ^{1}H NMR (600 MHz, $CDCl_3$): δ = 5.74 (s, *J* = 1.2 Hz, 1H, H2), 5.68 (s, 1H, -NH), 5.35 (quint., *J* = 2.9 Hz, 1H, H13), 4.71 (ddt, *J* = 11.6, 6.8, 1.8 Hz, 1H, H11), 3.80 (ddd, *J* = 9.0, 6.1, 1.1 Hz, 1H, H16), 3.79 (s, 1H, -OH), 3.47 (dd, *J* = 11.7, 8.9 Hz, 1H, H17a), 3.39 (dd, *J* = 11.7, 6.0 Hz, 1H, H17b), 2.90 (ddd, *J* = 12.7, 8.5, 8.0 Hz, 1H, H4a), 2.59 (dddd, *J* = 12.6, 7.3, 5.1, 1.0 Hz, 1H, H4b), 2.45 (m, 1H, H8), 2.33–2.37 (m, 2H, H5), 2.30 (ddt, *J* = 14.2, 3.1, 1.8 Hz, 1H, H12a), 2.10 (ddd, *J* = 14.7, 2.8, 2.0 Hz, 1H, H14a), 1.95 (dd, *J* = 14.7, 3.5 Hz, 1H, H14b), 1.87 (d, *J* = 1.4 Hz, H19, 3H), 1.44–1.67 (m, 4H, H9,

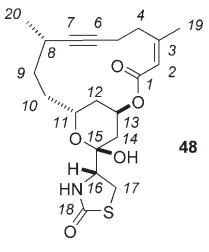

48

H10), 1.37 (ddd, $J=14.3$, 11.7, 2.6 Hz, 1H, H12b), 1.14 (d, $J=7.0$ Hz, 3H, H20); ^{13}C NMR (150 MHz, $CDCl_3$): $\delta=174.7$ (s, C18), 165.3 (s, C1), 156.1 (s, C3), 118.2 (d, C2), 97.7 (s, C15), 86.3 (s, C7), 79.6 (s, C6), 68.8 (d, C13), 63.9 (d, C11), 61.6 (d, C16), 34.1 (t, C10), 33.4 (t, C12), 32.7 (t, C4), 31.4 (t, C14), 31.3 (t, C9), 28.8 (t, C17), 25.6 (d, C8), 24.2 (q, C19), 22.7 (q, C20), 18.3 (t, C5).

Compound 50: Prepared as described above from ester **54** (12 mg, 0.022 mmol)[13] and CAN (30 mg, 0.054 mmol); colorless oil (4.5 mg, 49%). $[\alpha]_D^{20}=+11.5$ (c 0.41, CH_2Cl_2); ^{1}H NMR (400 MHz, CD_2Cl_2): $\delta=$ 6.42 (dt, $J=11.4$, 7.2 Hz, 1H), 5.86 (dt, $J=11.8$, 1.8 Hz, 1H), 5.73–5.68 (m, NH), 5.41 (quint., $J=3.0$ Hz, 1H), 4.10–4.02 (m, 1H, OH), 3.81 (ddd, $J=8.8$, 7.2, 1.0 Hz, 1H), 3.48 (dd, $J=11.6$, 8.8 Hz, 1H), 3.39 (dd, $J=11.7$, 6.3 Hz, 1H), 2.82 (qd, $J=7.2$, 1.8 Hz, 2H), 2.31–2.24 (m, 2H), 2.17–2.10 (m, 2H), 1.96 (d, $J=3.2$ Hz, 2H), 1.89 (dt, $J=14.4$, 2.4 Hz, 1H), 1.76 (t, $J=2.7$ Hz, 3H), 1.75 (t, $J=2.7$ Hz, 3H), 1.65–1.45 (m, 5H); ^{13}C NMR (75 MHz, CD_2Cl_2): $\delta=174.4$, 164.6, 150.8, 120.0, 97.6, 79.1, 78.0, 76.8, 76.0, 68.0, 65.3, 61.8, 35.0, 34.6, 31.8, 29.2, 29.0, 25.2, 18.9, 18.6, 3.5 (2C); IR (film): $\tilde{\nu}$ = 3333, 2919, 1677, 1416, 1164, 1091, 1063, 1016, 821 cm^{-1}; MS (EI): m/z (%): 419 (8), 317 (3), 179 (52), 161 (19), 133 (34), 121 (33), 111 (46), 102 (36), 93 (100), 77 (37); HRMS (ESI): m/z: calcd for $C_{22}H_{29}NO_5S+$Na: 442.16587; found: 442.16582 [M^++Na].

Compound 51: A solution of PPh_3 (16.5 mg, 0.063 mmol), DEAD (8.4 μL, 0.063 mmol), alcohol **17** (20 mg, 0.048 mmol)[13] and heptanoic acid (7.5 μL, 0.053 mmol) in benzene (2 mL) was stirred for 24 h before additional PPh_3 (50 mg, 0.15 mmol), DEAD (25 μL, 0.15 mmol) and heptanoic acid (23 μL, 0.15 mmol) were added. After 72 h reaction time, the solvent was evaporated and the residue was purified by flash chromatography (hexanes/EtOAc 2:1 → 1:1 → 1:2) to give ester **55** which was used in the next step without further characterization. CAN (40 mg, 0.074 mmol) was added to a solution of this ester (8 mg) in MeCN (0.45 mL) and water (0.22 mL) and the resulting mixture was stirred for 20 h at ambient temperature. The reaction mixture was partitioned between CH_2Cl_2 and water and the organic layer was dried over Na_2SO_4 and concentrated. Purification of the residue by flash chromatography (hexanes/EtOAc 2:1 → 1:1) gave product **51** as a colorless oil (2.8 mg, 14%). $[\alpha]_D^{20}=+30$ (c 0.25, CH_2Cl_2); ^{1}H NMR (400 MHz, C_6D_6): $\delta=5.72$ (s, NH), 5.07–5.03 (m, 1H), 4.16 (dd, $J=9.1$, 4.1 Hz, 1H), 4.05–3.97 (m, 1H), 3.92 (s, 1H), 3.79 (t, $J=9.0$ Hz, 1H), 3.22 (dd, $J=9.0$, 4.2 Hz, 1H), 2.43–2.35 (m, 1H), 1.95 (td, $J=7.6$, 3.5 Hz, 2H), 1.74–1.67 (m, 1H), 1.64–1.57 (m, 2H), 1.56 (d, $J=2.4$ Hz, 3H), 1.54–1.33 (m, 4H), 1.24–1.19 (m, 4H), 1.17 (d, $J=6.8$ Hz, 3H), 1.15–1.09 (m, 4H), 1.04–0.98 (m, 1H), 0.86 (t, $J=7.2$ Hz, 3H); ^{13}C NMR (75 MHz, C_6D_6): $\delta=171.4$, 159.5, 96.7, 83.7, 76.4, 68.0, 65.2, 64.7, 59.4, 34.5, 34.4, 33.7, 33.2, 32.1, 31.7, 29.0, 26.3, 25.2, 22.9, 21.9, 14.2, 3.5; IR (film): $\tilde{\nu}$ = 3348, 2921, 2858, 1740, 1407, 1241, 1170, 1097, 929, 803; MS (EI): m/z (%): 409 (5), 323 (3), 193 (89), 175 (27), 147 (46), 133 (75), 125 (60), 113 (42), 110 (11), 87 (34), 73 (52), 43 (100); HRMS (ESI): m/z: calcd for $C_{22}H_{35}NO_6$:+Na: 432.23566; found: 432.23584 [M^++Na].

X-Ray crystallographic study for compound 33: Data were recorded using an Bruker-AXS KappaCCD-diffractometer with graphite-monochromated $Mo_{K\alpha}$ radiation ($\lambda=0.71073$ Å). The crystal was mounted in a stream of cold nitrogen gas. The structures were solved by direct methods (SHELXS-97)[46] and refined by full-matrix least-squares techniques against F^2 (SHELXL-97).[47] Hydrogen atoms were inserted from geometry consideration using the HFIX option of the program. Selected data: $C_{28}H_{43}NO_6Si$, $M_r=517.72$ g mol^{-1}, colorless, crystal size $0.08\times0.06\times$ 0.04 mm, orthorhombic, $P2_12_12_1$ [No. 19], $a=7.2255(3)$, $b=12.6489(5)$, $c=32.6244(13)$ Å, $V=2981.7(2)$ Å^3, $Z=4$, $\rho_{calcd}=1.153$ Mg m^{-3}, $\mu=$ 0.117 mm^{-1}, $T=100$ K, 38101 reflections collected, 8662 independent reflections, 5823 reflections with $I>2\sigma(I)$, $\theta_{max}=30.01°$, 333 refined parameters, $R=0.067$, $wR^2=0.146$, $S=1.028$, largest diff. peak and hole $=0.6/-0.4$ e Å^{-3}.

CCDC-601356 contains the supplementary crystallographic data for this paper. These data can be obtained free of charge from The Cambridge Crystallographic Data Centre via www.ccdc.cam.ac.uk/data_request/cif/

Acknowledgements

Generous financial support by the MPG, the Chemical Genomics Center (CGC Initiative of the MPG), the Fonds der Chemischen Industrie, the Alexander-von-Humboldt Foundation (fellowships for M.D.B.F. and C.N.), and the Deutsch-Israelische Projektkooperation (DIP project) is gratefully acknowledged. We thank Dr. L. Parra-Rapado for the preparation of the bare macrocycle **52**, Dr. C. W. Lehmann for the crystal structure analysis of compound **33**, and Mrs. A. Langerak for excellent technical assistance.

[1] a) I. Spector, N. R. Shochet, Y. Kashman, A. Groweiss, *Science* **1983**, *219*, 493–495; b) review: I. Spector, N. R. Shochet, D. Blasberger, Y. Kashman, *Cell Motil. Cytoskeleton* **1989**, *13*, 127–144.

[2] a) A. Groweiss, U. Shmueli, Y. Kashman, *J. Org. Chem.* **1983**, *48*, 3512–3516; b) Y. Kashman, A. Groweiss, R. Lidor, D. Blasberger, S. Carmely, *Tetrahedron* **1985**, *41*, 1905–1914.

[3] a) J. R. Peterson, T. J. Mitchison, *Chem. Biol.* **2002**, *9*, 1275–1285; b) I. Spector, F. Braet, N. R. Shochet, M. R. Bubb, *Microsc. Res. Tech.* **1999**, *47*, 18–37; c) K. Ayscough, *Methods Enzymol.* **1998**, *298*, 18–25; d) T. M. A. Gronewold, F. Sasse, H. Lünsdorf, H. Reichenbach, *Cell Tissue Res.* **1999**, *295*, 121–129.

[4] a) I. Spector, N. R. Shochet, D. Blasberger, Y. Kashman, *J. Cell Biol.* **1986**, *103*, A393; b) K. A. El Sayed, D. T. A. Youssef, D. Marchetti, *J. Nat. Prod.* **2006**, *69*, 219–223.

[5] a) P. Sheterline, J. Clayton, J. C. Sparrow, *Actin*, 4th ed., Oxford University Press, New York, **1999**; b) T. D. Pollard, L. Blanchoin, R. D. Mullins, *Annu. Rev. Biophys. Biomol. Struct.* **2000**, *29*, 545–576; c) H. Lodish, D. Baltimore, A. Berk, S. L. Zipursky, P. Matsudaira, J. Darnell, *Molecular Cell Biology*, 3rd ed., Scientific American Books, New York, **1995**; d) A. Giganti, E. Friederich, in *Prog. Cell Cycle Res., Vol. 5* (Eds.: L. Meijer, A. Jézéquel, M. Roberge), Springer, Berlin, **2003**, pp. 511–523; e) G. Fenteany, S. Zhu, *Curr. Top. Med. Chem.* **2003**, *3*, 593–616; f) M. A. Jordan, L. Wilson, *Curr. Opin. Cell Biol.* **1998**, *10*, 123–130.

[6] W. M. Morton, K. R. Ayscough, P. J. McLaughlin, *Nat. Cell Biol.* **2000**, *2*, 376–378.

[7] See also: E. G. Yarmola, T. Somasundaram, T. A. Boring, I. Spector, M. R. Bubb, *J. Biol. Chem.* **2000**, *275*, 28120–28127.

[8] The non-basic endocyclic ester oxygen cannot serve as a hydrogen-bond acceptor.

[9] T. R. Hoye, S.-E. N. Ayyad, B. M. Eklov, N. E. Hashish, W. T. Shier, K. A. El Sayed, M. T. Hamann, *J. Am. Chem. Soc.* **2002**, *124*, 7405–7410.

[10] Note that Glu214 (E214) is erroneously assigned as D214 in ref. [6]. The structure deposited in the database (PDB ID: 1ESV) clearly identifies this residue as a glutamic acid moiety.

[11] A. Fürstner, D. De Souza, L. Turet, M. D. B. Fenster, L. Parra-Rapado, C. Wirtz, R. Mynott, C. W. Lehmann, *Chem. Eur. J.* **2006**, *12*, 115–134.

[12] Although previously practiced, the expression "diverted total synthesis" was coined only recently by Danishefsky. For a discussion and an instructive case, see: a) R. M. Wilson, S. J. Danishefsky, *J. Org. Chem.* **2006**, DOI: 10.1021/jo0610053; b) C. Gaul, J. T. Njardarson, D. Shan, D. C. Dorn, K.-D. Wu, W. P. Tong, X.-Y. Huang, M. A. S. Moore, S. J. Danishefsky, *J. Am. Chem. Soc.* **2004**, *126*, 11326–11337; c) short review: I. Paterson, E. A. Anderson, *Science* **2005**, *310*, 451–453; d) for a discussion of "natural product like" compounds and "natural product hybrids" see: L. F. Tietze, H. P. Bell, S. Chandrasekhar, *Angew. Chem.* **2003**, *115*, 4128–4160; *Angew. Chem. Int. Ed.* **2003**, *42*, 3996–4028.

[13] Preliminary communication: A. Fürstner, D. Kirk, M. D. B. Fenster, C. Aïssa, D. De Souza, O. Müller, *Proc. Natl. Acad. Sci. USA* **2005**, *102*, 8103–8108.

[14] Preliminary communications: a) A. Fürstner, D. De Souza, L. Parra-Rapado, J. T. Jensen, *Angew. Chem.* **2003**, *115*, 5516–5518; *Angew. Chem. Int. Ed.* **2003**, *42*, 5358–5360; b) A. Fürstner, L. Turet,

Angew. Chem. **2005**, *117*, 3528–3532; *Angew. Chem. Int. Ed.* **2005**, *44*, 3462–3466.

[15] a) A. Fürstner, R. Martin, *Chem. Lett.* **2005**, *34*, 624–629; b) B. Scheiper, M. Bonnekessel, H. Krause, A. Fürstner, *J. Org. Chem.* **2004**, *69*, 3943–3949; c) A. Fürstner, A. Leitner, M. Méndez, H. Krause, *J. Am. Chem. Soc.* **2002**, *124*, 13856–13863; d) A. Fürstner, A. Leitner, *Angew. Chem.* **2002**, *114*, 632–635; *Angew. Chem. Int. Ed.* **2002**, *41*, 609–612; e) G. Seidel, D. Laurich, A. Fürstner, *J. Org. Chem.* **2004**, *69*, 3950–3952.

[16] D. A. Evans, F. Urpi, T. C. Somers, J. S. Clark, M. T. Bilodeau, *J. Am. Chem. Soc.* **1990**, *112*, 8215–8216.

[17] a) J. Inanaga, K. Hirata, H. Saeki, T. Katsuki, M. Yamaguchi, *Bull. Chem. Soc. Jpn.* **1979**, *52*, 1989–1993; b) for advanced applications from this laboratory see: O. Lepage, E. Kattnig, A. Fürstner, *J. Am. Chem. Soc.* **2004**, *126*, 15970–15971; c) A. Fürstner, E. Kattnig, O. Lepage, *J. Am. Chem. Soc.* **2006**, *128*, 9194–9204; d) J. Mlynarski, J. Ruiz-Caro, A. Fürstner, *Chem. Eur. J.* **2004**, *10*, 2214–2222.

[18] For another instructive case in which an attempted Yamaguchi esterification of an α,β-unsaturated acid was unsuccessful see: a) A. Fürstner, C. Aïssa, C. Chevrier, F. Teplý, C. Nevado, M. Tremblay, *Angew. Chem.* **2006**, *118*, 5964–5969; *Angew. Chem. Int. Ed.* **2006**, *45*, 5832–5837; b) A. Fürstner, C. Nevado, M. Tremblay, C. Chevrier, F. Teplý, C. Aïssa, M. Waser, *Angew. Chem.* **2006**, *118*, 5969–5974; *Angew. Chem. Int. Ed.* **2006**, *45*, 5837–5842.

[19] O. Mitsunobu, *Synthesis* **1981**, 1–28.

[20] a) A. Fürstner, P. W. Davies, *Chem. Commun.* **2005**, 2307–2320; b) A. Fürstner, G. Seidel, *Angew. Chem.* **1998**, *110*, 1758–1760; *Angew. Chem. Int. Ed.* **1998**, *37*, 1734–1736.

[21] Applications of RCAM in natural product synthesis: a) A. Fürstner, K. Grela, C. Mathes, C. W. Lehmann, *J. Am. Chem. Soc.* **2000**, *122*, 11799–11805; b) A. Fürstner, K. Radkowski, J. Grabowski, C. Wirtz, R. Mynott, *J. Org. Chem.* **2000**, *65*, 8758–8762; c) A. Fürstner, A. Rumbo, *J. Org. Chem.* **2000**, *65*, 2608–2611; d) A. Fürstner, G. Seidel, *J. Organomet. Chem.* **2000**, *606*, 75–78; e) A. Fürstner, A.-S. Castanet, K. Radkowski, C. W. Lehmann, *J. Org. Chem.* **2003**, *68*, 1521–1528; f) A. Fürstner, C. Mathes, K. Grela, *Chem. Commun.* **2001**, 1057–1059; g) A. Fürstner, F. Stelzer, A. Rumbo, H. Krause, *Chem. Eur. J.* **2002**, *8*, 1856–1871; h) A. Fürstner, K. Grela, *Angew. Chem.* **2000**, *112*, 1292–1294; *Angew. Chem. Int. Ed.* **2000**, *39*, 1234–1236; i) D. Song, G. Blond, A. Fürstner, *Tetrahedron* **2003**, *59*, 6899–6904; j) B. Aguilera, L. B. Wolf, P. Nieczypor, F. P. J. T. Rutjes, H. S. Overkleeft, J. C. M. van Hest, H. E. Schoemaker, B. Wang, J. C. Mol, A. Fürstner, M. Overhand, G. A. van der Marel, J. H. van Boom, *J. Org. Chem.* **2001**, *66*, 3584–3589; k) N. Ghalit, A. J. Poot, A. Fürstner, D. T. S. Rijkers, R. M. J. Liskamp, *Org. Lett.* **2005**, *7*, 2961–2964; l) M. IJsselstijn, B. Aguilera, G. A. van der Marel, J. H. van Boom, F. L. van Delft, H. E. Schoemaker, H. S. Overkleeft, F. P. J. T. Rutjes, M. Overhand, *Tetrahedron Lett.* **2004**, *45*, 4379–4382; m) A. Fürstner, T. Dierkes, *Org. Lett.* **2000**, *2*, 2463–2465; n) A. Fürstner, C. Mathes, *Org. Lett.* **2001**, *3*, 221–223; o) J. Chan, T. F. Jamison, *J. Am. Chem. Soc.* **2004**, *126*, 10682–10691.

[22] a) A. Fürstner, C. Mathes, C. W. Lehmann, *J. Am. Chem. Soc.* **1999**, *121*, 9453–9454; b) A. Fürstner, C. Mathes, C. W. Lehmann, *Chem. Eur. J.* **2001**, *7*, 5299–5317.

[23] a) J. H. Freudenberger, R. R. Schrock, M. R. Churchill, A. L. Rheingold, J. W. Ziller, *Organometallics* **1984**, *3*, 1563–1573; b) A. Fürstner, O. Guth, A. Rumbo, G. Seidel, *J. Am. Chem. Soc.* **1999**, *121*, 11108–11113.

[24] a) The short supply has already led to first attempts to grow *N. magnifica* in aquaculture, cf. E. Hadas, M. Shpigel, M. Ilan, *Aquaculture* **2005**, *244*, 159–169; b) moreover, a recent study strongly suggests a non-symbiotic origin of latrunculin B, cf: O. Gillor, S. Carmeli, Y. Rahamim, Z. Fishelson, M. Ilan, *Mar. Biotechnol.* **2000**, *2*, 213–223.

[25] *CHARMM*, V. c31b1, **2004**.

[26] C. L. Brooks, M. Karplus, *J. Chem. Phys.* **1983**, *79*, 6312–6325.

[27] A. D. MacKerell, Jr., B. Brooks, C. L. Brooks, L. Nilsson, B. Roux, Y. Won, M. Karplus, in *Encyclopedia of Computational Chemistry, Vol. 1* (Ed.: P. von R. Schleyer), Wiley, Chichester, **1998**, pp. 271–277.

[28] *ChemShell*, V. 3.0a3, **2004**.

[29] P. Sherwood, et al., *THEOCHEM* **2003**, *632*, 1–28.

[30] W. Thiel, *MNDO99*, V. 6.1, Max-Planck-Institut für Kohlenforschung, Mülheim an der Ruhr (Germany), **2004**.

[31] K. Y. Burstein, A. N. Isaev, *Theor. Chim. Acta* **1984**, *64*, 397–401.

[32] M. J. S. Dewar, W. Thiel, *J. Am. Chem. Soc.* **1977**, *99*, 4899–4907.

[33] N. Foloppe, A. D. MacKerell, Jr., *J. Comput. Chem.* **2000**, *21*, 86–104.

[34] A. D. MacKerell, Jr, N. K. Banavali, *J. Comput. Chem.* **2000**, *21*, 105.

[35] A. D. MacKerell, Jr., D. Bashford, M. Bellott, R. L. Dunbrack, Jr., J. D. Evanseck, M. J. Field, S. Fischer, J. Gao, H. Guo, S. Ha, D. Joseph-McCarthy, L. Kuchnir, K. Kuczera, F. T. K. Lau, C. Mattos, S. Michnick, T. Ngo, D. T. Nguyen, B. Prodhom, W. E. Reiher, III, B. Roux, M. Schlenkrich, J. C. Smith, R. Stote, J. Straub, M. Watanabe, J. Wiorkiewicz-Kuczera, D. Yin, M. Karplus, *J. Phys. Chem. B* **1998**, *102*, 3586–3616.

[36] D. Bakowies, W. Thiel, *J. Phys. Chem.* **1996**, *100*, 10580–10594.

[37] A. H. de Vries, P. Sherwood, S. J. Collins, A. M. Rigby, M. Rigutto, G. J. Kramer, *J. Phys. Chem. B* **1999**, *103*, 6133–6141.

[38] There are H-bonds between the oxygen atoms of the macrocycle and surrounding waters, however, these will also be present in the solvent and should therefore have only a minor influence on the binding energy.

[39] Since the independent optimizations of the complexes are not directly comparable due to the distance criteria used in determining the active atoms during each optimization, the **2**/– and **44**/G-actin complexes were re-optimized for the sake of consistency. Using the **1**/G-actin complex as the starting point, the **2**/– and **44**/G-actin complexes were created by subsequently deleting the additional groups (i.e., for **2** the HC=CH linkage in the macrocycle, and then the methyl substituents to create the **44**/G-actin complex), followed by an optimization with smaller distance criteria (10 Å) for the active region (see Supporting Information for further details).

[40] L. R. Otterbein, P. Graceffa, R. Dominguez, *Science* **2001**, *293*, 708–711.

[41] J. A. McCammon, S. H. Northrup, *Nature* **1981**, *293*, 316–317.

[42] H.-X. Zhou, S. T. Wlodek, J. A. McCammon, *Proc. Natl. Acad. Sci. USA* **1998**, *95*, 9280–9283.

[43] M. P. Sibi, D. Rutherford, P. A. Renhowe, B. Li, *J. Am. Chem. Soc.* **1999**, *121*, 7509–7516.

[44] S. Ma, X. Lu, Z. Li, *J. Org. Chem.* **1992**, *57*, 709–713.

[45] a) U. S. Racherla, Y. Liao, H. C. Brown, *J. Org. Chem.* **1992**, *57*, 6614–6617; b) H. C. Brown, P. K. Jadhav, *J. Am. Chem. Soc.* **1983**, *105*, 2092–2093.

[46] G. M. Sheldrick, *SHELXS-97*, Program for the determination of crystal structures, University of Göttingen (Germany), **1997**.

[47] G. M. Sheldrick, *SHELXL-97*, Program for least-squares refinement of crystal structures, University of Göttingen (Germany), **1997**.

Received: September 19, 2006
Published online: November 8, 2006

